iPS cell generation from a patient with *KCNH2* mutation

To generate iPS cells, we used peripheral blood cells as donor somatic cells from the patient. Separated peripheral mononuclear cells were stimulated by CD3 antibody and IL-2 to activate T lymphocytes. And activated T lymphocytes were reprogrammed by using Sendai virus carrying *SOX2*, *OCT3/4* (also known as *POU5F1*), *KLF4*, and *MYC*. Several clones were generated, expanded and stored. All iPS cell lines showed typical iPS cell morphology and expressed human pluripotency markers (Fig. 2a and b). These iPS cells were moved to petri-dishes and formed embryoid bodies with spontaneous beating, which indicated that these patient-specific iPS cells properly differentiated into beating cardiomyocytes *in vitro*.

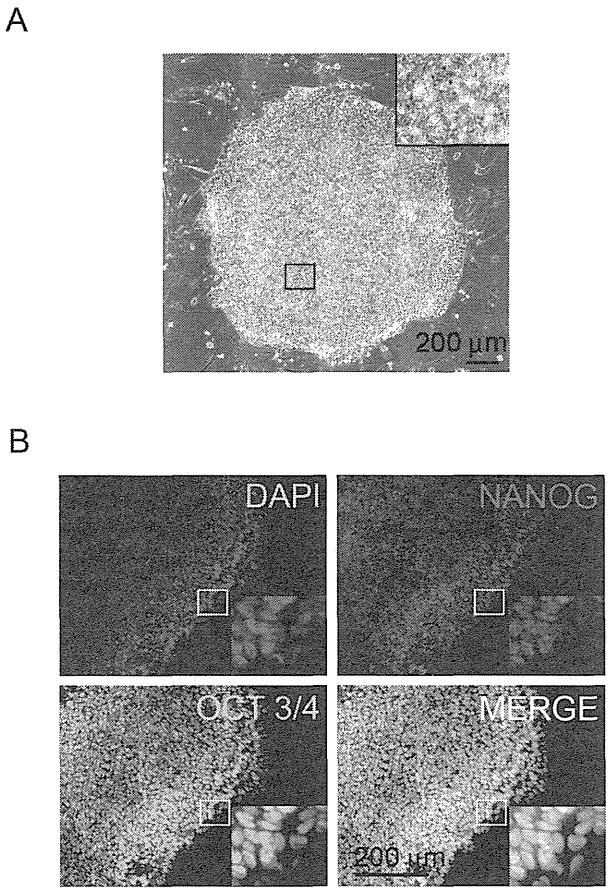

Figure 2. Generation of iPS cells from the patient with *KCNH2* G603D (G1808A) mutation.
A. Representative phase-contrast image of patient-specific iPS cell colony. Black box in figure is shown at a higher magnification in the inset. **B.** Immunofluorescence staining for stem cell markers (OCT3/4, NANOG and DAPI) in the patient-specific iPS cell colony. White boxes in each figure are shown at a higher magnification in the inset.

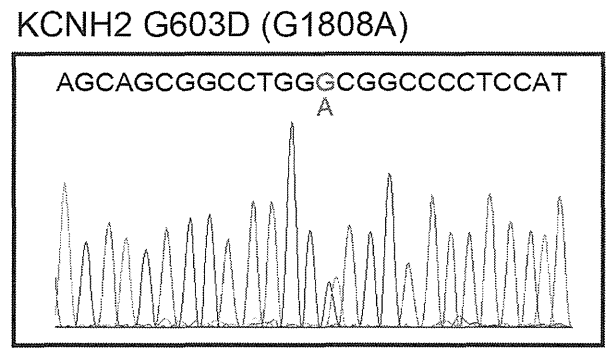

Figure 3. Novel *KCNH2* mutation in the patient-specific iPS cell colony.
Sequence analysis of genomic *KCNH2* in the patient-specific iPS cell colony. The novel *KCNH2* G603D (G1808A) mutation.

KCNH2 mutation in iPS cells derived from a patient with *KCNH2* mutation

To confirm that the generated iPS cells have a same mutation as the patient has, the genotype analysis was performed. It revealed the *KCNH2* G603D (G1808A) mutation was taken over (Figure 3).

Discussion

In the present study, we successfully generated iPS cells from a patient with the *KCNH2* G603D mutation who didn't exhibit any symptoms but showed prolonged QT interval at ECG. This patient is still young and may exhibit the cardiac symptom in the future. In real clinical setting, it is very important to know whether patients with genetic mutation will develop severe diseases or not. If we can predict the severity in the future disease manifestation, we can easily determine to do those patients, e.g., intensive care, exercise limitation, no medication and so on. So it is valuable to establish patient-specific disease model and develop the systems to evaluate the characteristics of patient-specific diseases. Patient-specific iPS cells may contribute to these concepts.

In terms of disease modeling using iPS cells, LQT2 is firstly noticed[13-15] because LQT2 is one of the most common genetic variants in long QT syndrome and there is no definitive therapy for LQT2. And drug discovery often failed at the expense of immense cost, due to the side effects related to HERG which is LQT2 associated gene product, following QT prolongation and lethal arrhythmia. First report showed the generation of LQT2 patient-specific iPS cells harboring A614V missense mutation in the *KCNH2* gene, which was previously shown to lead to a significant reduction of

IKr which is responsible for LQT2[15]. Detailed whole-cell patch-clamp and multi-electrode array (MEA) recordings revealed significant prolongation of the action potential duration in LQT2 iPS cell-derived cardiomyocytes. Voltage-clamp studies confirmed a significant reduction of the cardiac potassium current IKr. LQT2 iPS cell-derived cardiomyocytes also showed marked arrhythmogenicity, characterized by early-after depolarizations (EAD) and triggered arrhythmias. And calcium-channel blockers, K_{ATP}-channel openers and late sodium channel blockers ameliorate the disease phenotype in LQT2 iPS cell-derived cardiomyocyte. Second report showed the generation of LQT2 patient-specific iPS cells harboring G1681A missense mutation in the *KCNH2* gene, which was also previously shown to lead to a significant reduction of IKr[14]. MEA and patch-clamp recording showed prolonged field/action potential duration in LQT2 iPS cell-derived cardiomyocytes. LQT2 iPS cell-derived cardiomyocytes developed EADs when challenged with the E4031 (IKr blocker) and isoprenaline. Action potential duration and EAD were ameliorated by propranolol, nadolol, nicorandil and an activator of hERG, PD118057. The other report showed the generation of LQT2 patient-specific iPS cells harboring R176W missense mutation in the *KCNH2* gene[13]. The *KCNH2* R176W mutation is relatively common variant and was reported to have the frequency of 0.5% in apparently healthy individuals. Although there were some reports showed that this mutation was related to long QT syndrome, the majority of these individuals were completely asymptomatic and unaware of their carrier status, as is the case with this patient. In heterologous expression system, R176W reduced hERG tail current density by ~75%, but upon coexpression with wild type the difference in current densities was nullified. But the action potential duration of LQT2 iPS cell-derived cardiomyocytes was significantly longer than that of control, and IKr density of the LQT2 iPS cell-derived cardiomyocytes was significantly reduced. Consistent with clinical observations, the LQT2 iPS cell-derived cardiomyocytes demonstrated a more pronounced inverse correlation between the beating rate and repolarization time compared with control cells. Additionally, LQT2 iPS cell-derived cardiomyocytes were more sensitive than controls to potentially arrhythmogenic drugs, including sotalol, and demonstrated arrhythmogenic electrical activity.

In this study we chose a patient with a novel mutation in the *KCNH2* G603D. Patient showed QT interval prolongation but never showed any symptoms. To treat properly and prevent cardiac lethal arrhythmia, we believe it is valuable to generate experimental methods to predict how susceptible to lethal arrhythmia in various stimulations in those patients. Actually, many genomic variations such as many SNPs in each patient's genome affect disease manifestation even in the patients with major functional mutation and may be the cause of low penetrance for long QT syndrome[16]. So it is difficult to accurately predict disease susceptibility only by genomic information such as patient's mutation and SNPs. Patient-specific iPS cells have all genomic information encoded in patient's genome including mutation and all SNPs, and can be ideal disease models for the patients. Actually, each patient shows different disease phenotype and drug response, which is also partly due to patient genomic variation. In terms of personalized medicine, we can also try many notorious and beneficial drugs on patient-specific iPS cell-derived cardiomyocyte and predict disease susceptibility before the patient will use those drugs. To generate patient-specific disease models using iPS cells, we established the patient-specific iPS cells and confirmed the patient-specific iPS cells had the same mutation as the patient.

Acknowledgments

The authors thank all the laboratory members for their critical comments and helpful discussions.

References

1. Takahashi K, Yamanaka S. Induction of Pluripotent Stem Cells from Mouse Embryonic and Adult Fibroblast Cultures by Defined Factors. Cell. 2006; 126(4): 663-76.
2. Takahashi K, Tanabe K, Ohnuki M, et al. Induction of Pluripotent Stem Cells from Adult Human Fibroblasts by Defined Factors. Cell. 2007; 131(5): 861-72.
3. Seki T, Yuasa S, Oda M, et al. Generation of Induced Pluripotent Stem Cells from Human Terminally Differentiated Circulating T Cells. Cell Stem Cell. 2010; 7(1): 11-4.
4. Egashira T, Yuasa S, Fukuda K. Induced pluripotent stem cells in cardiovascular medicine. Stem Cells Int. 2011; 2011: 348960.
5. Yuasa S, Fukuda K. Recent advances in cardiovascular regenerative medicine: the induced pluripotent stem cell era. Expert Rev Cardiovasc Ther. 2008 Jul; 6(6): 803-10.
6. Yuasa S, Fukuda K. Cardiac regenerative medicine. Circ J. 2008; 72 Suppl A: A49-55.
7. Egashira T, Yuasa S, Suzuki T, et al. Disease characterization using LQTS-specific induced pluripotent stem cells. Cardiovasc Res. 2012 Sep 1; 95(4): 419-29.
8. Horigome H, Nagashima M, Sumitomo N, et al. Clinical characteristics and genetic background of congenital

long-QT syndrome diagnosed in fetal, neonatal, and infantile life: a nationwide questionnaire survey in Japan. Circ Arrhythm Electrophysiol. 2010 Feb; 3(1): 10-7.
9. Shimizu W, Horie M. Phenotypic manifestations of mutations in genes encoding subunits of cardiac potassium channels. Circ Res. 2011 Jun 24; 109(1): 97-109.
10. Giudicessi JR, Ackerman MJ. Potassium-channel mutations and cardiac arrhythmias—diagnosis and therapy. Nat Rev Cardiol. 2012; 9(6): 319-32.
11. Seki T, Yuasa S, Fukuda K. Generation of induced pluripotent stem cells from a small amount of human peripheral blood using a combination of activated T cells and Sendai virus. Nat Protoc. 2012 Apr; 7(4): 718-28.
12. Seki T, Yuasa S, Fukuda K. Derivation of Induced Pluripotent Stem Cells from Human Peripheral Circulating T Cells. Current Protocols in Stem Cell Biology: John Wiley & Sons, Inc.; 2011.
13. Lahti AL, Kujala VJ, Chapman H, et al. Model for long QT syndrome type 2 using human iPS cells demonstrates arrhythmogenic characteristics in cell culture. Dis Model Mech. 2012 Mar; 5(2): 220-30.
14. Matsa E, Rajamohan D, Dick E, et al. Drug evaluation in cardiomyocytes derived from human induced pluripotent stem cells carrying a long QT syndrome type 2 mutation. Eur Heart J. 2011 Apr; 32(8): 952-62.
15. Itzhaki I, Maizels L, Huber I, et al. Modelling the long QT syndrome with induced pluripotent stem cells. Nature. 2011; 471(7337): 225-9.
16. Priori SG, Schwartz PJ, Napolitano C, et al. Risk stratification in the long-QT syndrome. N Engl J Med. 2003 May 8; 348(19): 1866-74.

Induction of human cardiomyocyte-like cells from fibroblasts by defined factors

Rie Wada[a], Naoto Muraoka[a,b], Kohei Inagawa[a,b], Hiroyuki Yamakawa[a,b], Kazutaka Miyamoto[a,b], Taketaro Sadahiro[a,b], Tomohiko Umei[a], Ruri Kaneda[a,b], Tomoyuki Suzuki[b,c], Kaichiro Kamiya[c], Shugo Tohyama[b], Shinsuke Yuasa[b], Kiyokazu Kokaji[d], Ryo Aeba[d], Ryohei Yozu[d], Hiroyuki Yamagishi[e], Toshio Kitamura[f], Keiichi Fukuda[b], and Masaki Ieda[a,b,g,1]

[a]Department of Clinical and Molecular Cardiovascular Research and [b]Department of Cardiology, School of Medicine, Keio University, Tokyo 160-8582, Japan; [c]Department of Cardiovascular Research, Research Institute of Environmental Medicine, Nagoya University, Nagoya 464-8601, Japan; [d]Division of Cardiovascular Surgery and [e]Department of Pediatrics, School of Medicine, Keio University, Tokyo 160-8582, Japan; [f]Division of Cellular Therapy, Institute of Medical Science, University of Tokyo, Tokyo 108-8639, Japan; and [g]Japan Science and Technology Agency CREST, Tokyo 160-8582, Japan

Edited by Margaret Buckingham, Pasteur Institute, Paris, France, and approved June 11, 2013 (received for review March 6, 2013)

Heart disease remains a leading cause of death worldwide. Owing to the limited regenerative capacity of heart tissue, cardiac regenerative therapy has emerged as an attractive approach. Direct reprogramming of human cardiac fibroblasts (HCFs) into cardiomyocytes may hold great potential for this purpose. We reported previously that induced cardiomyocyte-like cells (iCMs) can be directly generated from mouse cardiac fibroblasts in vitro and vivo by transduction of three transcription factors: Gata4, Mef2c, and Tbx5, collectively termed GMT. In the present study, we sought to determine whether human fibroblasts also could be converted to iCMs by defined factors. Our initial finding that GMT was not sufficient for cardiac induction in HCFs prompted us to screen for additional factors to promote cardiac reprogramming by analyzing multiple cardiac-specific gene induction with quantitative RT-PCR. The addition of Mesp1 and Myocd to GMT up-regulated a broader spectrum of cardiac genes in HCFs more efficiently compared with GMT alone. The HCFs and human dermal fibroblasts transduced with GMT, Mesp1, and Myocd (GMTMM) changed the cell morphology from a spindle shape to a rod-like or polygonal shape, expressed multiple cardiac-specific proteins, increased a broad range of cardiac genes and concomitantly suppressed fibroblast genes, and exhibited spontaneous Ca^{2+} oscillations. Moreover, the cells matured to exhibit action potentials and contract synchronously in coculture with murine cardiomyocytes. A 5-ethynyl-2′-deoxyuridine assay revealed that the iCMs thus generated do not pass through a mitotic cell state. These findings demonstrate that human fibroblasts can be directly converted to iCMs by defined factors, which may facilitate future applications in regenerative medicine.

cell fate conversion | regeneration | cardiogenesis

Cardiovascular disease remains a leading cause of death worldwide, for which current therapeutic regimens remain limited. Given that adult human hearts have little regenerative capacity after injury, the demand is high for cardiac regenerative therapy. The recent discovery of induced pluripotent stem cells (iPSCs) allows the direct generation of specific cell types from differentiated somatic cells by overexpression of lineage-specific factors.

Several previous studies have demonstrated that such direct lineage reprogramming can yield a diverse range of cell types, including pancreatic β cells, neurons, neural progenitors, blood progenitors, and hepatocyte-like cells (1–5). We previously reported that a minimum mixture of three cardiac-specific transcription factors—Gata4, Mef2c, and Tbx5 (GMT)—directly induced cardiomyocyte-like cells (iCMs) from mouse fibroblasts in vitro (6). Following our report, three other groups also reported generation of functional cardiomyocytes from mouse fibroblasts with various combinations of transcription factors, either with GMT plus Hand2 (GHMT) or Mef2c, Myocd, and Tbx5 or using microRNAs (7–9). Although full reprogramming into beating cardiomyocytes was not efficient in vitro (10, 11), gene transfer of GMT or GHMT into mouse hearts generated new cardiomyocytes from endogenous cardiac fibroblasts and improved cardiac function after myocardial infarction (7, 12, 13). The foregoing studies suggest that direct cardiac reprogramming may be a useful therapeutic approach for regenerative purposes, and that identification of reprogramming factors in human cells is important for the development of this technology (14–16).

In the present study, we sought to generate cardiomyocytes directly from postnatal human fibroblasts. We found that GMT was not sufficient for cardiac reprogramming in human cells. We then screened additional reprogramming factors for their ability to induce cardiac reprogramming by analyzing multiple cardiac gene induction, and found that the addition of Mesp1 and Myocd to GMT was able to generate cardiomyocyte-like cells from human fibroblasts in vitro.

Results

Gata4, Mef2c, Tbx5, Mesp1, and Myocd Induce Multiple Cardiac Gene Expression in Human Cardiac Fibroblasts. We first developed a culture system for human cardiac fibroblasts (HCFs) following our mouse cardiac fibroblast isolation protocol. Human atrial tissues were obtained from 36 patients (age 1 mo to 80 y; average age, 35 y) undergoing cardiac surgery with informed consent following the guidelines of the Keio University Ethics Committee. The $Thy1^+/CD31^-$ FACS-sorted fibroblasts did not express cardiomyocyte or cardiac progenitor cell (CPC) genes, but did express fibroblast genes on quantitative RT-PCR (qRT-PCR) analysis (Fig. S1 *A*–*C*). HCFs expressed fibroblast proteins, vimentin, and fibronectin, but not markers of cardiomyocytes, CPCs, smooth muscle cells, or endothelial cells (Fig. 1*A* and Fig. S1*D*). The antibody immunoreactivities were confirmed in the positive controls (Fig. S1*E*). FACS analyses also demonstrated that the HCF population did not contaminate cardiomyocytes (Fig. 1*B*).

For transduction, we first used the sequential lentivirus/ecotropic retrovirus infection following the iPSC generation protocol from human dermal fibroblasts (HDFs) (17). The transduction efficiency was <20% in HCFs (Fig. 1*C*). We then directly infected HCFs using other types of retroviruses, produced by PLAT-A cells and PLAT-GP cells (18). We achieved high transduction efficiency

Author contributions: M.I. designed research; R.W., N.M., K.I., K.M., T. Suzuki, S.Y., R.A., and M.I. performed research; T. Sadahiro, T.U., S.T., K. Kokaji, R.Y., and T.K. contributed new reagents/analytic tools; H. Yamakawa, R.K., T. Suzuki, K. Kamiya, H. Yamagishi, K.F., and M.I. analyzed data; and M.I. wrote the paper.

The authors declare no conflict of interest.

This article is a PNAS Direct Submission.

[1]To whom correspondence should be addressed. E-mail: mieda@z8.keio.jp.

This article contains supporting information online at www.pnas.org/lookup/suppl/doi:10.1073/pnas.1304053110/-/DCSupplemental.

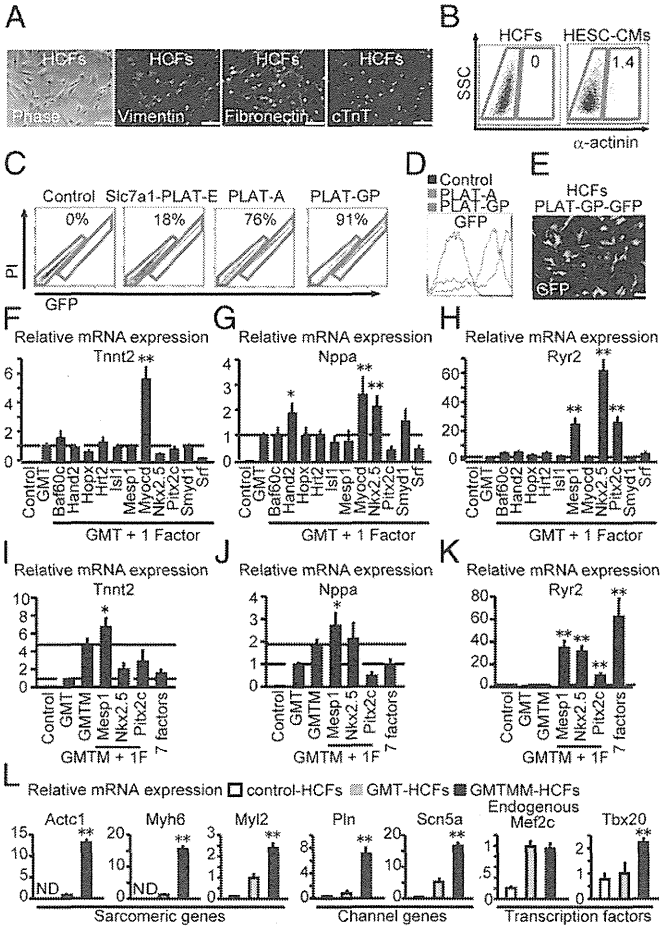

Fig. 1. Gata4, Mef2c, Tbx5, Mesp1, and Myocd induce cardiac gene expression in HCFs. (*A*) Morphology and characterization of HCFs by phase-contrast imaging, with vimentin, fibronectin, and cTnT immunostaining [passage number 1 (P1) HCFs, 57-y-old patient; $n = 3$]. The antibody immunoreactivities were confirmed in HESC-CMs (Fig. S1*E*). (*B*) FACS analysis for α-actinin$^+$ cells (HESC-CMs as a positive control) showed no expression in HCFs (P1 HCFs, 58-y-old patient; $n = 3$). (*C*) FACS analysis of the HCFs transduced by sequential infection of Slc7a1 lentivirus and ecotropic GFP retrovirus (Slc7a1-PLAT-E), amphotropic GFP retrovirus produced by PLAT-A cells (PLAT-A), and pantropic GFP retrovirus produced by PLAT-GP cells (PLAT-GP) (P1 HCFs from patients aged 1 mo and 50 y; $n = 4$). (*D*) Histogram of GFP intensity in the transduced HCFs determined by FACS analysis (P1 HCFs from 50-y-old patient; $n = 3$). GFP expression was high in cells transduced with retrovirus produced by PLAT-GP. (*E*) Image of HCFs infected by the GFP retrovirus produced by PLAT-GP. (*F–H*) mRNA expression of cardiac genes (*Tnnt2*, *Nppa*, and *Ryr2*) in HCFs transduced with GMT plus individual factors as determined by qRT-PCR after 1 wk of transduction (P1 HCFs, 71-y-old patient; $n = 3$). Data were normalized against the GMT values. See also Fig. S2 *A–E* and Movie S1. (*I–K*) The mRNA expression of cardiac genes in HCFs transduced with GMTM plus Mesp1, Nkx2.5, Pitx2c, or all three genes was determined by qRT-PCR after 1 wk of transduction (P1 HCFs, 59-y-old patient; $n = 3$). Data were normalized against the GMT values. (*L*) Multiple cardiac genes were up-regulated in GMTMM-HCFs after 1 wk of transduction (P1 HCFs, 2-y-old patient; $n = 3$). Representative data are shown in each panel. All data are presented as mean ± SD. $^*P < 0.05$; $^{**}P < 0.01$ vs. relevant control. (Scale bars: 100 μm.)

(>90%) using the pantropic retrovirus from PLAT-GP cells, and used this virus in subsequent experiments (Fig. 1 *C–E*).

We next transduced HCFs with a mixture of GMT retroviruses. The GMT overexpression induced very few α-actinin$^+$ cells, suggesting that this mixture is insufficient for human cardiac reprogramming (Fig. 2*A*). To identify reprogramming factors, we screened an additional 11 factors for use in combination with GMT and analyzed the induction of multiple cardiac genes by qRT-PCR after 1 wk of transduction. Of these 11 factors, only Myocd strongly induced *Tnnt2* expression (Fig. 1*F*). Myocd also induced *Nppa*, but did not induce *Ryr2* (ryanodine receptor 2). In contrast, Mesp1, Nkx2.5, and Pitx2c strongly induced *Ryr2* expression (Fig. 1 *G* and *H*).

Consistent with our qRT-PCR results, FACS analysis and immunocytochemistry demonstrated that the addition of Myocd to GMT increased the expression of sarcomere proteins α-actinin and cTnT in HCFs compared with Mesp1. In contrast, threefold more cells exhibited spontaneous Ca^{2+} oscillations by transduction of GMTMesp1 compared with GMTMyocd after 4 wk of culture (Fig. S2 *A–E* and Movie S1).

We next investigated whether the addition of Mesp1, Nkx2.5, or Pitx2c to GMT and Myocd could induce multiple cardiac gene expression. We found that Nkx2.5 and Pitx2c inhibited *Tnnt2* mRNA expression, but that addition of Mesp1 up-regulated all three cardiac genes (Fig. 1 *I–K*). Moreover, transduction of Gata4, Mef2c, Tbx5, Mesp1, and Myocd (GMTMM) up-regulated the expression of a panel of cardiac genes related to different functions, including sarcomere structure, ion channels, and transcription factors, compared with GMT or mock infection, suggesting a more comprehensive reprogramming by GMTMM than by GMT (Fig. 1*L*).

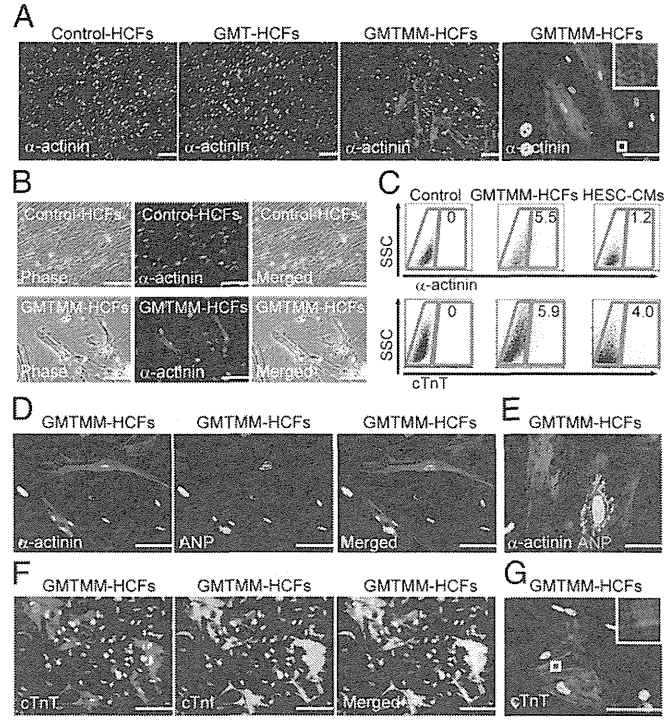

Fig. 2. Generation of cardiomyocyte-like cells from HCFs with GMTMM. (*A*) Immunostaining for α-actinin and DAPI in HCFs and GMT- or GMTMM-transduced HCFs at 4 wk after transduction (P1 HCFs, 3-y-old patient; $n = 4$). Note that GMTMM induced abundant and strong α-actinin expression. (*Inset*) High-magnification view of the area in the white box showing sarcomeric organization (see Fig. S1*E* for a positive control). (*B*) Morphology of mock- and GMTMM-infected HCFs by phase-contrast imaging and with α-actinin immunostaining (P1 HCFs, 57-y-old patient; $n = 3$). (*C*) Quantitative data of α-actinin$^+$ (P1 HCFs, 3-mo-old patient; $n = 3$) and cTnT$^+$ (P1 HCFs, 5-mo-old patient; $n = 3$) cells in GMTMM-HCFs and HESC-CMs ($n = 3$). (*D* and *E*) GMTMM-HCFs expressed both α-actinin and ANP at 4 wk after transduction (P1 HCFs, 5-y-old patient; $n = 2$). ANP was expressed at the perinuclear site. (*F* and *G*) Induced cardiomyocyte-like cells expressed cTnT and cTnI at 8 wk after GMTMM transduction (P1 HCFs, 5-y-old patient; $n = 2$). (Inset) High-magnification view representing the area in the white box. Representative data are shown in each panel. (Scale bars: 100 μm in *A*, *B*, *D*, *F*, and *G*; 50 μm in *E*.)

Gata4, Mef2c, Tbx5, Mesp1, and Myocd Induce Cardiac-Specific Proteins and Sarcomeric Structures in HCFs. We next used immunocytochemistry to examine whether cardiac proteins were expressed in HCFs by GMTMM. We found that more GMTMM-transduced HCFs (GMTMM-HCFs) expressed α-actinin with higher intensity compared with GMT, and that the α-actinin$^+$ cells had sarcomere-like structures after 4 wk of culture (Fig. 2*A*). Morphologically, mock-infected HCFs were spindle-shaped, whereas GMTMM-HCFs appeared thicker and refractive on phase-contrast microscopy, with a polygonal or rod-like shape (Fig. 2*B*). FACS analysis demonstrated that approximately 5% of the GMTMM-HCFs expressed the endogenous cardiac proteins α-actinin and cTnT (Fig. 2*C*). In addition to α-actinin, the GMTMM-HCFs expressed several cardiomyocyte-specific proteins, including atrial natriuretic peptide (ANP), cTnT, cTnI, and connexin 43 (Cx43), at similar levels as those in the human ES cell-derived cardiomyocytes (HESC-CMs) (Fig. 2 *D–G* and Figs. S1*E* and S2*F*). Approximately 40% of α-actinin$^+$ cells expressed ANP, and most cTnT$^+$ cells expressed cTnI, another cardiomyocyte-specific sarcomere protein (Fig. 2 *D–G*). The addition of Nkx2.5 reduced cTnT expression, confirming the qRT-PCR results (Fig. 1*I* and Fig. S2*G*). These findings suggest that GMTMM induces multiple cardiac proteins and cardiomyocyte-like structures in HCFs.

GMTMM Up-Regulates a Broad Range of Cardiac Genes and Suppresses Fibroblast Gene Expression. Next, to decipher the global transcriptional changes induced by GMTMM transduction, we investigated the gene expression profiles of HCFs, GMTMM-HCFs, and hearts by microarray analyses. We analyzed the mRNA expression of GMTMM-HCFs after 1 wk of infection at the early reprogramming stage, because we were not able to isolate human iCM populations from GMTMM-HCFs, and the percentage of iCMs relative to the total number of GMTMM-HCFs decreased over time owing to their loss of proliferative capacity. Among the 24,462 genes analyzed, 1,432 genes were differentially expressed by more than twofold between HCFs and GMTMM-HCFs, with 1,018 genes up-regulated and 414 genes down-regulated in GMTMM-HCFs (Fig. 3*A*). The genes up-regulated in GMTMM-HCFs were significantly enriched in hearts compared with HCFs (P = 1.6E-86) and, conversely, the down-regulated genes were enriched in fibroblasts (P = 4.7E-67) (Fig. 3*B*).

Gene Ontology (GO) analyses demonstrated that the genes up-regulated in GMTMM-HCFs were enriched related to cardiomyocyte functions, whereas the down-regulated genes were enriched for fibroblast functions, including cell division, mitotic cell cycle, cell proliferation, and cell adhesion (Fig. 3*C*). Heatmap and qRT-PCR analyses of a panel of cardiac and fibroblast genes in HCFs, GMTMM-HCFs, and hearts revealed that GMTMM up-regulated cardiac genes and concomitantly suppressed fibroblast gene expression (Fig. 3 *D* and *E*).

GMTMM Directly Induces Cardiomyocyte-Like Cells from Fibroblasts. We next asked whether GMTMM also could induce smooth muscle cells or endothelial cells from fibroblasts. Microarray and qRT-PCR analyses revealed induction of smooth muscle genes, but not endothelial cell genes, in GMTMM-HCFs (Fig. 4 *A* and *B*). Consistent with this finding, immunostaining demonstrated that CD31 was not expressed in GMTMM-HCFs, whereas calponin and smooth muscle myosin heavy chain (SMMHC), markers for smooth muscle cells, and α-smooth muscle actin (α-SMA), a marker of smooth muscles and embryonic cardiomyocytes (19), were induced by GMTMM transduction (Fig. 4 *C* and *D* and Fig. S3*A*). Coimmunostaining revealed that α-actinin$^+$ cells expressed α-SMA but not SMMHC, suggesting that the iCMs were relatively immature cardiomyocytes without a mixed phenotype between cardiomyocytes and smooth muscle cells (Fig. 4 *E–G*).

We next examined the reprogramming kinetics by analyzing the cardiomyocyte and smooth muscle cell gene induction by

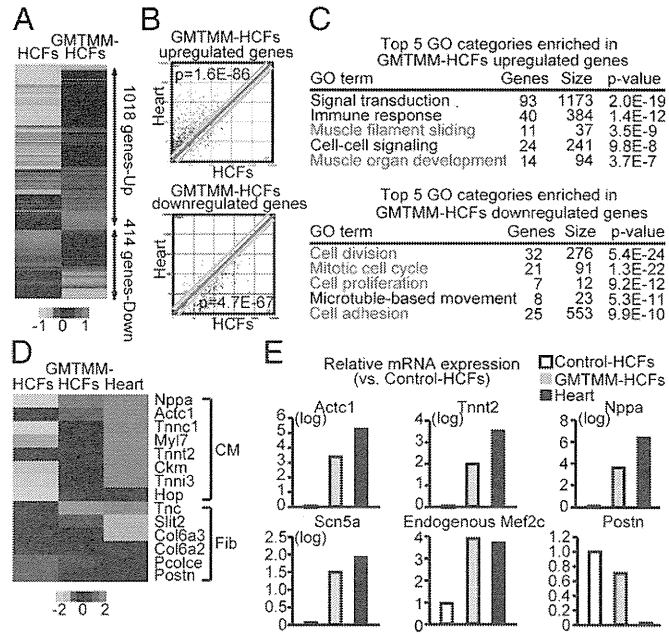

Fig. 3. GMTMM up-regulates cardiac genes and down-regulates fibroblast genes. (*A*) Heatmap image of microarray data, illustrating differentially expressed genes between control-HCFs and GMTMM-HCFs (P1 HCFs, 65-y-old patient; n = 1). The scale is −1 to +1 in log10. Red indicates increased expression, and green indicates decreased expression. "Up" indicates the genes up-regulated in GMTMM-HCFs compared with HCFs, and "down" indicates the genes down-regulated by GMTMM transduction compared with HCFs. (*B*) Paired scatterplots of the up-regulated and down-regulated genes in the GMTMM-HCFs. The up-regulated genes were significantly enriched in heart, whereas the down-regulated genes were enriched in HCFs. (*C*) GO term analyses of the up-regulated and down-regulated genes in GMTMM-HCFs compared with HCFs. The top five GO categories are shown. (*D*) Heatmap image of gene expression of cardiomyocyte (CM)- and fibroblast (Fib)-enriched genes in HCFs, GMTMM-HCFs, and heart. The scale is −2 to +2 in log10. (*E*) mRNA expression in HCFs, GMTMM-HCFs, and heart were determined by qRT-PCR (P1 HCFs, 2-y-old patient; n = 3). Data were normalized against the control-HCF values. All data are presented as mean, and the scales are log10 in Actc1, Tnnt2, Nppa, and Scn5 mRNA expression (*E*).

qRT-PCR. The cardiomyocyte-specific genes *Actc1*, *Nppa*, *Ryr2*, and *Tnnt2* and smooth muscle-specific gene *Myh11* were up-regulated from 4 d and subsequently down-regulated at 28 d by GMTMM, because these reprogrammed myocytes were not proliferative (Fig. 4*H*). We then performed 5-ethynyl-2′-deoxyuridine (EdU) incorporation assays to determine whether the conversion of fibroblasts to cardiomyocyte-like and smooth muscle-like cells is mediated through a mitotic cell state. A 2-hr pulse labeling of EdU after 4 or 24 h of transduction demonstrated significantly reduced cell proliferation in the GMTMM-HCFs, consistent with the GO term analysis results (Fig. S3 *B–D*). Long-term pulse labeling of EdU throughout a 4-wk culture period demonstrated that a vast majority of α-actinin$^+$ and SMMHC$^+$ cells did not express EdU. These results suggest that most induced cardiac and smooth muscle cells do not pass through a mitotic cell state and start to express cardiac or smooth muscle genes from the early stage of reprogramming (Fig. 4 *I–K*).

Induced Cardiomyocyte-Like Cells Exhibit Action Potentials and Contractile Ability in Coculture with Murine Cardiomyocytes. To determine whether the iCMs derived from HCFs have the functional properties of cardiomyocytes, we analyzed intracellular Ca^{2+} oscillations after 4 wk of culture. We did not observe Ca^{2+} oscillations in mock-infected HCFs. In contrast, approximately 1% of GMTMM-HCFs showed spontaneous Ca^{2+} oscillations, albeit

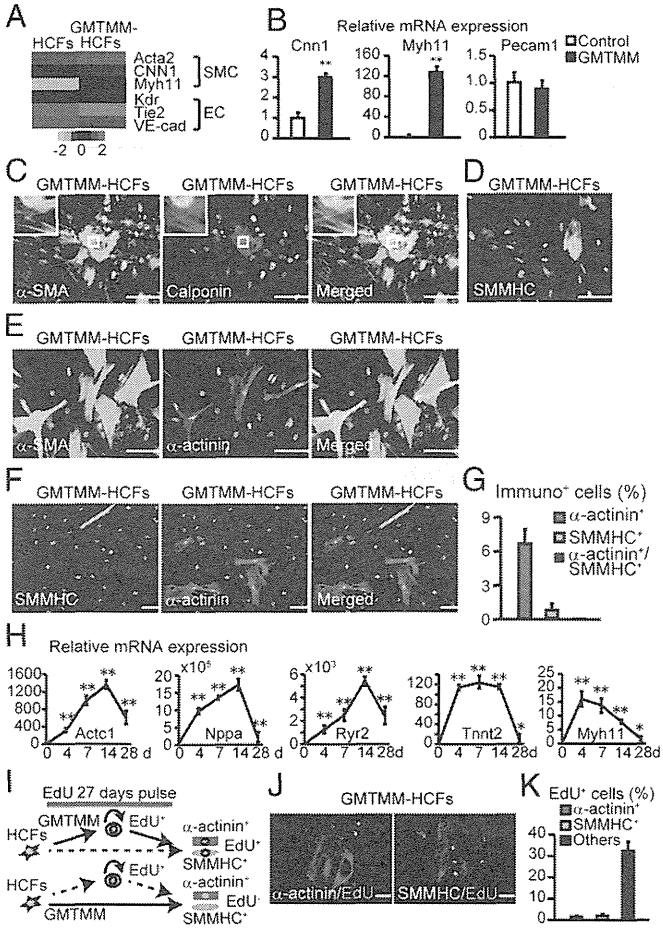

Fig. 4. Generation of induced cardiomyocyte-like cells is not mediated through mitotic cells. (*A*) Heatmap image of gene expression of smooth muscle cell (SMC)- and endothelial cell (EC)-enriched genes in HCFs and GMTMM-HCFs (P1 HCFs, 65-y-old patient; $n = 1$). The scale is −2 to +2 in log10. (*B*) mRNA expression in control-HCFs and GMTMM-HCFs as determined by qRT-PCR (P1 HCFs, 2-y-old patient; $n = 3$). (*C*) Coimmunostaining for α-SMA and calponin in the GMTMM-HCFs (P1 HCFs, 50-y-old patient, $n = 3$). (*D*) Immunostaining for SMMHC in the GMTMM-HCFs (P1 HCFs, 80-y-old patient; $n = 3$). See also Fig. S1*E*. (*E*) Coimmunostaining for α-SMA and α-actinin in the GMTMM-HCFs (P1 HCFs, 5-mo-old patient; $n = 3$). (*F* and *G*) Double immunostaining for SMMHC and α-actinin in the GMTMM-HCFs, along with quantitative data for α-actinin$^+$ cells, SMMHC$^+$ cells, and α-actinin$^+$/SMMHC$^+$ cells (P1 HCFs, 5-mo-old patient; $n = 3$). (*H*) Time course of mRNA expression in GMTMM-HCFs at day 0 and at 4, 7, 14, and 28 d after infection, determined by qRT-PCR (P2 HCFs, 6-y-old patient; $n = 3$). (*I*) Schematic representation of EdU treatment on HCFs during reprogramming. (*J* and *K*) Immunocytochemistry for α-actinin and SMMHC in GMTMM-HCFs at 28 d after infection, coupled with EdU incorporation. The majority of immunopositive cells were negative for EdU. Quantitative data are shown in *K* (P1 HCFs, 1-y-old patient; $n = 3$). All data are presented as mean ± SD. $^*P < 0.05$; $^{**}P < 0.01$ vs. relevant control. (Scale bars: 100 μm.)

at a lower frequency compared with HESC-CMs (Fig. 5 *A–D* and Movies S2 and S3). Despite longer periods of culture, the GMTMM-HCFs did not beat spontaneously. Consequently, we next tested whether coculture with murine cardiomyocytes could induce further cardiac maturation. We transduced HCFs with GMTMM and GFP by separate vectors or GFP alone to mark the transduced cells, and after 1 wk of transduction, replated the cells onto neonatal rat cardiomyocytes. We found expression of cardiac markers, such as α-actinin, cTnT, and Cx43, in the GMTMM/GFP-HCFs, but not in the GFP-HCFs (Fig. 5*E* and Fig. S4 *A–C*). After 7 d of cocultivation, 5% of the GMTMM/GFP$^+$ cells contracted synchronously with surrounding cardiomyocytes; however, conditioned media from rat cardiomyocytes did not induce spontaneous contraction in the GMTMM-transduced cells. The beating iCMs revealed periodic Ca oscillations and action potentials (APs) similar to those of HESC-CMs (Fig. 5 *F–J* and Movie S4) (20). Atrial-like APs were the most frequently recorded in the HCF-iCMs ($n = 27$; 0 nodal type, 19 atrial type, and 8 ventricular type) (Fig. 5*J*). Of note, we injected Alexa Fluor 568 dye into the patched cells and confirmed that the recorded electrical activities came from the GMTMM/GFP$^+$ iCMs (Fig. 5*H*).

Next, to investigate cell fusion events, we transduced GMTMM and DsRed retrovirus mixtures into the HCFs and cocultured with GFP-labeled cardiomyocytes. Cellular contraction was apparent in DsRed$^+$ cells but not in DsRed$^+$/GFP$^+$ cells, suggesting that cell

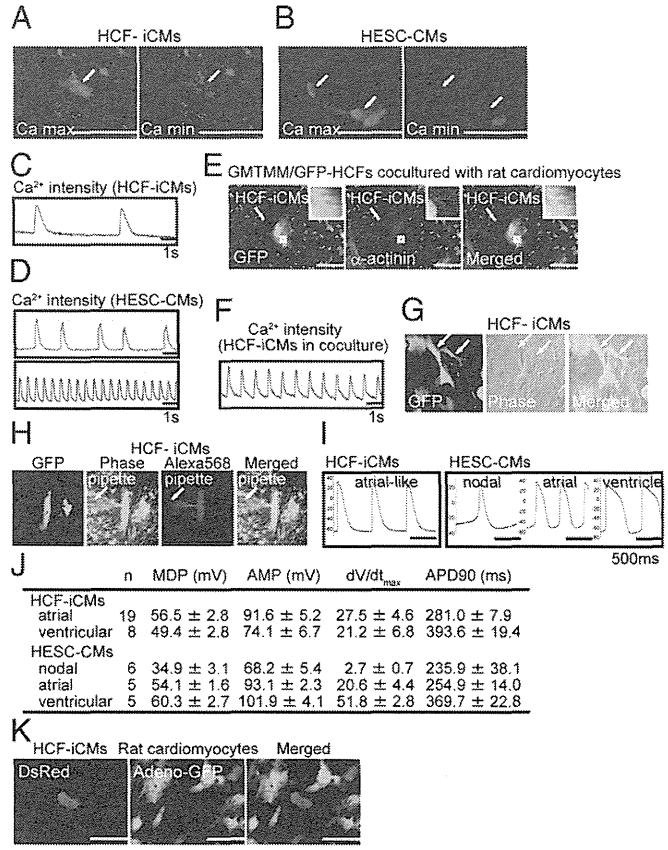

Fig. 5. Functional analyses of induced cardiomyocyte-like cells derived from HCFs. (*A* and *B*) Spontaneous Ca^{2+} oscillations were observed in HCF-iCMs (arrows in *A*) and HESC-CMs (arrows in *B*) (P1 HCFs, 5-mo-old patient; $n = 3$). Rhod-3 signals at maximum and minimum Ca^{2+} are shown. See also Movie S2. (*C* and *D*) HCF-iCMs showing spontaneous Ca^{2+} oscillation (*C*), similar to HESC-CMs (*D*; see also Movie S3). Rhod-3 intensity traces are shown. (*E*) Immunocytochemisty for α-actinin in the GMTMM/GFP-expressing HCF-iCMs (P2 HCFs, 57-y-old; $n = 2$) cocultured with rat cardiomyocytes. See also Fig. S4 *A–C*. (*F* and *G*) iCMs cocultured with rat neonatal cardiomyocytes showing Ca^{2+} oscillations (P1 HCFs, 77-y-old patient; $n = 2$). See also Movie S4. (*H*) APs recorded from iCMs (P1 HCFs, 57-y-old, 1-y-old, and 4-y-old patients; $n = 27$). The cells were injected with Alexa Fluor 568 to confirm that APs were obtained from the GFP$^+$ iCMs. (*I*) APs from HCF-iCMs and HESC-CMs. HESC-CMs revealed variable APs. (*J*) Summary of the measured AP parameters. MDP, maximum diastolic potential; AMP, amplitude; dV/dt, maximum rate of rise of AP; APD90, AP duration at 90% of repolarization. P1 HCFs from 57-y-old, 1-y-old, and 4-y-old patients were used for the experiments in the HCF-iCMs ($n = 27$). (*K*) HCF-iCMs (DsRed) cocultured with rat cardiomyocytes (GFP) (P1 HCFs, 17-y-old patient; $n = 4$). The DsRed$^+$ cell is beating without cell fusion. See also Fig. S4*D* and Movies S5 and S6. All data are presented as mean ± SEM. Representative data are shown in each panel. (Scale bars: 100 μm in *A*, *B*, *E*, and *K*.)

fusion was unlikely for cardiac differentiation in the coculture (Fig. 5*K*, Fig. S4*D*, and Movies S5 and S6).

Induction of Human Cardiomyocyte-Like Cells from Dermal Fibroblasts. To exclude the possibility of contamination with rare CPCs or cardiomyocytes in our initial fibroblast populations, we tested whether HDFs also could be converted into iCMs by GMTMM. Neonatal foreskin dermal fibroblasts transduced with GMTMM expressed α-actinin, cTnT, and ANP and showed sarcomeric structures (Fig. 6 *A* and *B*). FACS analysis revealed that most HDFs were Thy1$^+$/CD31$^-$ fibroblasts, which also expressed cardiac genes after GMTMM transduction (Fig. S5 *A* and *B*). GMTMM-HDFs expressed cardiac-specific genes at levels comparable to GMTMM-HCFs on qRT-PCR analysis (Fig. 6*C*). Microarray analyses of HDFs, GMTMM-HDFs, and hearts demonstrated that the up-regulated genes in the GMTMM-HDFs were cardiac-enriched genes (P = 1.2E-21) and the down-regulated genes were fibroblast-enriched genes (P = 1.5E-74) (Fig. 6*D* and Fig. S5*C*). The top five GO categories enriched in the up-regulated genes included muscle contraction and muscle filament sliding (Fig. S5*D*). A panel of cardiac-specific genes, including *Actc1*, *Tnnc1*, *Nppa*, *Nppb*, *Myl7*, *Pln* (phospholamban), and *Ckm*, were up-regulated, whereas fibroblast genes *Col3a1*, *Col6a3*, *Col16a1*, *Ecm2*, *Ptn*, and *Tnc* were down-regulated in GMTMM-HDFs (Fig. 6*E*). We also observed that some GMTMM-HDFs exhibited cellular contraction and APs in coculture with murine cardiomyocytes (n = 6, nodal/atrial/ventricular type = 0/2/4) (Fig. 6 *F*, *G*, and *K*; Fig. S5 *E* and *F*; and Movie S7). These results exclude the possibility that the iCMs arose from contaminating cardiomyocytes or CPCs in initial fibroblast populations.

We next used a doxycycline-inducible system to assess the requirement for exogenous reprogramming factors in maintaining a cardiac phenotype in iCMs. We found that transduction efficiency was ~70%, and that transgene expression was instantly diminished by withdrawal of doxycycline, with complete loss after 10 d (Fig. S5*G*). Expression of GMTMM for 5 wk induced α-actinin and cTnT expression in HCFs (Fig. 6*H* and Fig. S5*H*). We then withdrew doxycycline after 1 wk, 10 d, or 2 wk of induction, and cultured the cells for 3 wk without doxycycline. Doxycycline removal after 1 wk and 10 d did not induce cardiac reprogramming, whereas 2 wk of induction maintained endogenous α-actinin and cTnT expression in the iCMs, and the cells exhibited APs in coculture with murine cardiomyocytes (n = 7; 0 nodal type, 7 atrial type, 0 ventricular type) (Fig. 6 *H–K* and Fig. S5*I*). These results suggest that the fibroblasts were stably converted into cardiomyocyte-like cells after 2 wk of GMTMM transduction.

Discussion

Here we demonstrate that human fibroblasts can be directly converted to cardiomyocyte-like cells by overexpression of defined factors. We found that a pantropic retrovirus was more efficient for transduction into HCFs compared with amphotropic or lentivirus/ecotropic retrovirus systems. Given that high transduction efficiency is critical for reprogramming, the pantropic retrovirus might be widely useful for direct reprogramming from difficult-to-infect cells (11).

Compared with mouse counterparts, induction of human iCMs required two additional factors, Mesp1 and Myocd. Generation of human iPSCs and neuronal cells also required different culture conditions or other transcription factors in addition to the mouse reprogramming factors (21, 22). Mesp1 is expressed in CPCs and programs nascent mesoderm toward a cardiovascular cell fate, whereas Myocd regulates the development of cardiomyocytes and smooth muscle cells (23–25). Islas et al. (26) recently reported that overexpression of Ets2 and Mesp1 reprogrammed HDFs into CPCs, and that the induced CPCs differentiated into immature cardiomyocytes. Mesp1 overexpression activated some of the core cardiac transcription factors but failed to convert fibroblasts to CPCs. Given that their induced CPCs were highly replicative cells, the route of cardiac induction by Ets2/Mesp1 differed from that by GMTMM. More recently, Nam et al. (27) reported that overexpression of Gata4, Hand2, Tbx5, Myocd, miR-1, and miR-133 reprogrammed human fibroblasts into cardiac-like myocytes. Consistent with our results, they also found that neither of the mouse reprogramming factors GHMT or GMT was sufficient for cardiac reprogramming in human fibroblasts, and that the addition of Myocd significantly increased the expression of cardiac sarcomeric proteins. In addition, they reported that Hand2 was critical for inducing tropomyosin and cTnT in HDFs, and that

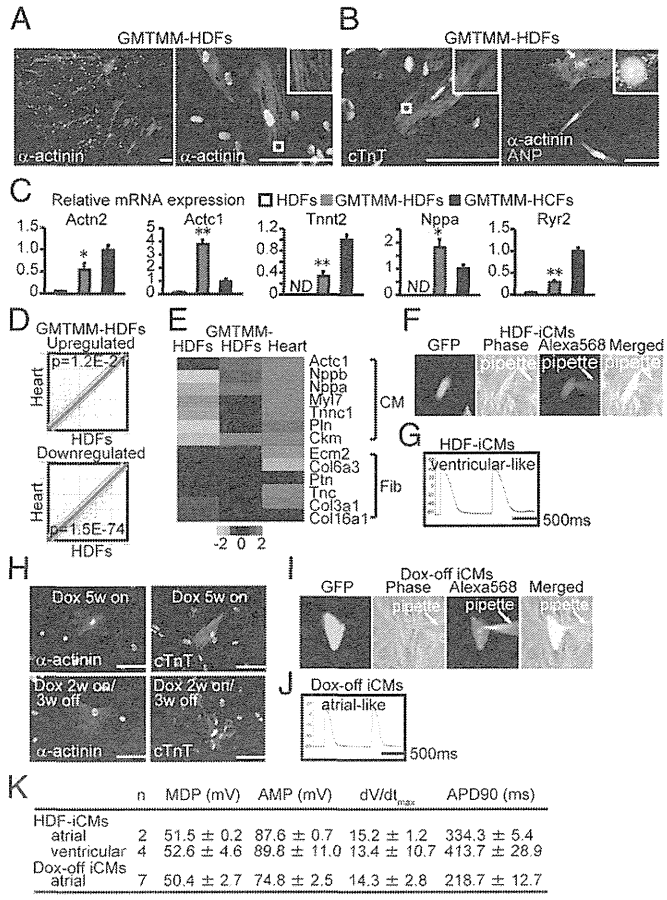

K

	n	MDP (mV)	AMP (mV)	dV/dt_{max}	APD90 (ms)
HDF-iCMs					
atrial	2	51.5 ± 0.2	87.6 ± 0.7	15.2 ± 1.2	334.3 ± 5.4
ventricular	4	52.6 ± 4.6	89.8 ± 11.0	13.4 ± 10.7	413.7 ± 28.9
Dox-off iCMs					
atrial	7	50.4 ± 2.7	74.8 ± 2.5	14.3 ± 2.8	218.7 ± 12.7

Fig. 6. GMTMM converts HDFs into cardiomyocyte-like cells. (*A*) Immunocytochemistry for α-actinin in GMTMM-HDFs at 4 wk after transduction (P3 HDFs; n = 3). (*B*) Immunocytochemistry revealing cTnT and ANP expression in GMTMM-HDFs (P3 HDFs; n = 3). (*Insets*) High-magnification views. (*C*) mRNA expression of cardiac genes in HDFs, GMTMM-HDFs (P3 HDFs), and GMTMM-HCFs as determined by qRT-PCR (n = 3). (*D*) Plots of gene expression up-regulated and down-regulated by more than twofold by GMTMM transduction in HDFs (P3 HDFs; n = 1). See also Fig. S5 *C* and *D*, heatmap image of microarray data and GO analyses. (*E*) Heatmap image of gene expression for cardiomyocyte (CM)- and fibroblast (Fib)-enriched genes in HDFs, GMTMM-HDFs, and heart. (*F* and *G*) APs recorded from GMTMM/GFP-expressing HDF-iCMs cocultured with rat cardiomyocytes (P3 HDFs; n = 6). The cells were injected with Alexa Fluor 568. Quantitative data are shown in *K*. See also Fig. S5 *E* and *F* and Movie S7. (*H*) (*Upper*) Immunostaining for α-actinin and cTnT in iCMs at 5 wk after Dox induction of the lentivirus. (*Lower*) Cells after 2 wk of Dox administration and 3 wk of Dox withdrawal (P1HCFs, 50-y-old patient; n = 2). See also Fig. S5 *G–I*. (*I–K*) APs recorded from iCMs at 2 wk after Dox withdrawal of the lentivirus (Dox-off iCMs) in coculture with cardiomyocytes (P1HCFs, 6-y-old patient; n = 7). Quantitative data are shown in *K*. Representative data are shown in each panel. Data are presented as mean ± SD in *C* and as mean ± SEM in *K*. *P < 0.05; **P < 0.01 vs. GMTMM-transduced HCFs. (Scale bars: 100 μm in *A*, *B*, and *H*.)

CELL BIOLOGY

the addition of miR-1 and 133 further improved cardiac reprogramming and eliminated the requirement for Mef2c.

In their study, by transduction using the six factors, 13% of adult HCFs expressed cTnT and a small subset of the cells exhibited spontaneous contractions after 11 wk of culture, suggesting greater reprogramming efficiency than with GMTMM. However, the functional properties of the induced cardiac-like myocytes remain unclear, and further investigation may be needed to clarify this point. Myocd overexpression induces smooth muscle cells from fibroblasts by forming transcriptional complexes with Srf and promotes cardiomyocyte differentiation by interacting with Gata4 and Tbx5 (28–30). Stoichiometry of transcription factors might determine the cell fate of GMTMM-transduced cells to iCMs or smooth muscle-like cells in our study. As demonstrated by the fact that addition of Myocd upregulated sarcomeric genes and Mesp1 induced intracellular Ca^{2+} oscillations, Myocd and Mesp1 differentially regulate cardiac gene expression in human cardiac reprogramming.

The human iCMs generated by GMTMM seem to be relatively immature cardiomyocytes, as indicated by their cell morphology, expression of embryonic cardiomyocyte marker α-SMA, and slow Ca^{2+} oscillations. Compared with mouse iCMs, human iCMs require coculture with murine cardiomyocytes to differentiate into beating cardiomyocytes. In this sense, the human iCMs may be similar to the early stage of embryonic cardiomyocytes before the start of contraction. Alternatively, the cells might be partially reprogrammed cardiomyocytes, much like the pre-iPSCs that can become fully pluripotent with additional stimuli.

Although the iCMs expressed a panel of cardiac-specific genes, their similarity of human iCMs to bona fide cardiomyocytes remained unclear. To address this question, we attempted to FACS-sort iCM populations using a fluorescent dye that labels mitochondria to selectively mark cardiomyocytes in ESC culture (31); however, we could not use this dye owing to the abundant labeling of mitochondria in the nonconverted HCF population. Further study is needed to thoroughly optimize conditions for human iCM generation and maturation and characterize the properties of iCMs.

It is possible that the immature iCM phenotypes could reflect the low percentage of iCMs and low cell–cell contact in the heterogeneous culture, and that enrichment of iCMs may enhance cardiac reprogramming. Given that secreted proteins, electrical and mechanical stimulation, and cell–cell contact might promote cardiac differentiation and reprogramming in the coculture, the in vitro system might represent a valuable platform for screening such key factors. From a practical standpoint, GMTMM may be sufficient human cardiac reprogramming factors, considering that the in vivo environment might be more permissive than culture dishes for reprogramming (7, 13). Further in vitro and in vivo studies are needed to facilitate application of this technology in potential regenerative therapies.

Materials and Methods

Human atrial tissues were obtained from 36 patients undergoing cardiac surgery (age 1 mo to 80 y; average age, 35 y) with informed consent in conformation with the guidelines of the Keio University Ethics Committee. HCFs were obtained following the mouse protocol as detailed in *SI Materials and Methods*. Human neonatal foreskin dermal fibroblasts (DS Pharma Biomedical) were cultured in DMEM containing 10% FBS. All experiments were performed using fibroblasts of early passage number (P1–P3). The Keio Centre for Clinical Research approved all of the experiments in this study (20100131). Isolation of human fibroblasts, cell culture, retroviral and lentiviral infection, FACS analysis, immunocytochemistry, qRT-PCR, DNA microarray, calcium imaging, and patch clamp electrophysiology are described in *SI Materials and Methods*.

Note Added in Proof. Nam et al. (27) reported that overexpression of Gata4, Hand2, Tbx5, Myocd, miR-1, and miR-133 reprogrammed human fibroblasts into cardiac-like myocytes. We found that a different combination of cardiac reprogramming factors– Gata4, Mef2c, Tbx5, Mesp1, and Myocd–also reprogrammed human fibroblasts into cardiomyocyte-like cells. Our induced cardiomyocytes did not beat spontaneously, but matured to exhibit action potentials and contract synchronously in coculture with murine cardiomyocytes.

ACKNOWLEDGMENTS. We are grateful to members of the K.F. laboratory, S. Miyoshi, K. Okamoto, M. Kudo, H. Shimizu, T. Oyanagi, K. Tomita, and medical staff at the Division of Cardiovascular Surgery and Department of Pediatrics, Keio University School of Medicine, and patients who agreed to participate in this project. M.I. was supported by research grants from Japan Science and Technology Agency CREST, Japan Society for the Promotion of Science, Banyu Life Science, the Uehara Memorial Foundation, Kimura Memorial Heart Foundation, Japan Research Foundation for Clinical Pharmacology, and Senshin Medical Research Foundation.

1. Zhou Q, Brown J, Kanarek A, Rajagopal J, Melton DA (2008) In vivo reprogramming of adult pancreatic exocrine cells to beta-cells. *Nature* 455(7213):627–632.
2. Vierbuchen T, et al. (2010) Direct conversion of fibroblasts to functional neurons by defined factors. *Nature* 463(7284):1035–1041.
3. Sekiya S, Suzuki A (2011) Direct conversion of mouse fibroblasts to hepatocyte-like cells by defined factors. *Nature* 475(7356):390–393.
4. Lujan E, Chanda S, Ahlenius H, Südhof TC, Wernig M (2012) Direct conversion of mouse fibroblasts to self-renewing, tripotent neural precursor cells. *Proc Natl Acad Sci USA* 109(7):2527–2532.
5. Szabo E, et al. (2010) Direct conversion of human fibroblasts to multilineage blood progenitors. *Nature* 468(7323):521–526.
6. Ieda M, et al. (2010) Direct reprogramming of fibroblasts into functional cardiomyocytes by defined factors. *Cell* 142(3):375–386.
7. Song K, et al. (2012) Heart repair by reprogramming non-myocytes with cardiac transcription factors. *Nature* 485(7400):599–604.
8. Jayawardena TM, et al. (2012) MicroRNA-mediated in vitro and in vivo direct reprogramming of cardiac fibroblasts to cardiomyocytes. *Circ Res* 110(11):1465–1473.
9. Protze S, et al. (2012) A new approach to transcription factor screening for reprogramming of fibroblasts to cardiomyocyte-like cells. *J Mol Cell Cardiol* 53(3):323–332.
10. Chen JX, et al. (2012) Inefficient reprogramming of fibroblasts into cardiomyocytes using Gata4, Mef2c, and Tbx5. *Circ Res* 111(1):50–55.
11. Srivastava D, Ieda M (2012) Critical factors for cardiac reprogramming. *Circ Res* 111(1):5–8.
12. Inagawa K, et al. (2012) Induction of cardiomyocyte-like cells in infarct hearts by gene transfer of Gata4, Mef2c, and Tbx5. *Circ Res* 111(9):1147–1156.
13. Qian L, et al. (2012) In vivo reprogramming of murine cardiac fibroblasts into induced cardiomyocytes. *Nature* 485(7400):593–598.
14. Hansson EM, Chien KR (2012) Reprogramming a broken heart. *Cell Stem Cell* 11(1):3–4.
15. Palpant NJ, Murry CE (2012) Regenerative medicine: Reprogramming the injured heart. *Nature* 485(7400):585–586.
16. Inagawa K, Ieda M (2013) Direct reprogramming of mouse fibroblasts into cardiac myocytes. *J Cardiovasc Transl Res* 6(1):37–45.
17. Takahashi K, et al. (2007) Induction of pluripotent stem cells from adult human fibroblasts by defined factors. *Cell* 131(5):861–872.
18. Kitamura T, et al. (2003) Retrovirus-mediated gene transfer and expression cloning: Powerful tools in functional genomics. *Exp Hematol* 31(11):1007–1014.
19. Kruithof BP, Van Den Hoff MJ, Tesink-Taekema S, Moorman AF (2003) Recruitment of intra- and extracardiac cells into the myocardial lineage during mouse development. *Anat Rec A Discov Mol Cell Evol Biol* 271(2):303–314.
20. He JQ, Ma Y, Lee Y, Thomson JA, Kamp TJ (2003) Human embryonic stem cells develop into multiple types of cardiac myocytes: Action potential characterization. *Circ Res* 93(1):32–39.
21. Pang ZP, et al. (2011) Induction of human neuronal cells by defined transcription factors. *Nature* 476(7359):220–223.
22. Yu J, et al. (2007) Induced pluripotent stem cell lines derived from human somatic cells. *Science* 318(5858):1917–1920.
23. Bondue A, et al. (2008) Mesp1 acts as a master regulator of multipotent cardiovascular progenitor specification. *Cell Stem Cell* 3(1):69–84.
24. Huang J, et al. (2012) Myocardin regulates BMP10 expression and is required for heart development. *J Clin Invest* 122(10):3678–3691.
25. Hoofnagle MH, et al. (2011) Myocardin is differentially required for the development of smooth muscle cells and cardiomyocytes. *Am J Physiol Heart Circ Physiol* 300(5):H1707–H1721.
26. Islas JF, et al. (2012) Transcription factors ETS2 and MESP1 transdifferentiate human dermal fibroblasts into cardiac progenitors. *Proc Natl Acad Sci USA* 109(32):13016–13021.
27. Nam YJ, et al. (2013) Reprogramming of human fibroblasts toward a cardiac fate. *Proc Natl Acad Sci USA* 110(14):5588–5593.
28. Oh J, et al. (2004) Target gene-specific modulation of myocardin activity by GATA transcription factors. *Mol Cell Biol* 24(19):8519–8528.
29. Wang C, Cao D, Wang Q, Wang DZ (2011) Synergistic activation of cardiac genes by myocardin and Tbx5. *PLoS ONE* 6(8):e24242.
30. Wang Z, Wang DZ, Pipes GC, Olson EN (2003) Myocardin is a master regulator of smooth muscle gene expression. *Proc Natl Acad Sci USA* 100(12):7129–7134.
31. Hattori F, et al. (2010) Nongenetic method for purifying stem cell-derived cardiomyocytes. *Nat Methods* 7(1):61–66.
32. Ieda M, et al. (2009) Cardiac fibroblasts regulate myocardial proliferation through beta1 integrin signaling. *Dev Cell* 16(2):233–244.

Generation of induced pluripotent stem cells from a small amount of human peripheral blood using a combination of activated T cells and Sendai virus

Tomohisa Seki[1], Shinsuke Yuasa[1,2] & Keiichi Fukuda[1]

[1]Department of Cardiology, Keio University School of Medicine, Tokyo, Japan. [2]Department of Cardiology, Center for Integrated Medical Research, Keio University School of Medicine, Tokyo, Japan. Correspondence should be addressed to K.F. (kfukuda@sc.itc.keio.ac.jp) or S.Y. (yuasa@a8.keio.jp).

Published online 15 March 2012; doi:10.1038/nprot.2012.015

Induced pluripotent stem cells (iPSCs) have become important cell sources for genetic disease models, and they have the potential to be cell sources for future clinical therapies. However, invasive tissue sampling reduces the number of candidates who consent to donate cells for iPSC generation. In addition, integrated transgenes can potentially insert at inappropriate points in the genome, and in turn have a direct oncogenic effect. Technical modifications using a combination of activated T cells and a temperature-sensitive mutant of Sendai virus (SeV) can avoid invasive tissue sampling and residual transgene issues in generating iPSCs. Such advances may increase the number of consenting patients for cell donations. Here we present a detailed protocol for the generation of iPSCs from a small amount of human peripheral blood using a combination of activated T cells and mutant SeV encoding human OCT3/4, SOX2, KLF4 and c-MYC; T cell–derived iPSCs can be generated within 1 month of blood sampling.

INTRODUCTION

Generating iPSCs is a prominent recent advance in stem cell biology[1]. iPSCs have become cell sources for genetic disease models and are expected to provide important new cell sources for clinical therapies. Initial studies generated human iPSCs from human fibroblasts obtained from dermal biopsy samples[2,3]. However, although further studies successfully reprogrammed several types of human somatic cells into iPSCs[4–6], the methods and cell sources most suitable for iPSC applications in humans remain undetermined. In particular, the generation of iPSCs for disease research should ideally avoid invasive tissue sampling, which markedly reduces the number of patients who consent to cell donations. In this regard, peripheral blood is an appealing cell source because of the noninvasive collection and easy accessibility of blood cells compared with skin fibroblasts and other types of cells from adult tissues.

We recently demonstrated that transgene-free iPSCs can be efficiently generated from a small amount of human peripheral blood within 1 month of the blood sampling using a combination of activated T cells and temperature-sensitive (TS) mutants of SeV encoding human OCT3/4, SOX2, KLF4 and c-MYC (**Fig. 1**)[7]. We named these T cell–derived iPSCs TiPS cells (TiPSCs). Recombinant SeVs that replicate in the cytoplasm of infected cells in the form of negative-sense single-stranded RNA were originally used to generate iPSCs from human fibroblasts[8]. These recombinant SeVs do not integrate into the host genome[9], and have already been used in human iPSC generation using $CD34^+$ cells from human cord blood[10]. Introducing TS mutations also successfully erased residual genomic RNA of the SeV vectors from the target cells[10], thus generating transgene-free iPSCs with high efficiency. T cells are also an appealing cell source because they are easily proliferated *in vitro* using a plate-bound anti-CD3 monoclonal antibody and interleukin (IL)-2 (ref. 11). Although it was reported that T cells are not efficiently reprogrammed using only four factors in the mouse[12,13], SeV vectors were efficiently transduced into human activated T cells to express exogenous genes[14]. Thus, the combination of activated T cells and TS SeV mutants made it possible to generate TiPSCs from patients effectively, easily and less invasively.

Advantages of the method

The initial methods for generating human iPSCs used a skin biopsy[2,3], requiring local anesthesia and suturation. In our protocol, iPSCs can be generated from patients without such invasive tissue sampling. Sufficient patient-specific iPSCs can be generated from 1 ml or less of peripheral blood, which contains sufficient terminally differentiated T cells[7]. Our method might therefore decrease the likelihood of patients refusing cell sampling and therefore potentially increase the number of patients who consent to generating iPSCs. In addition, TiPSCs can still be generated from whole blood samples stored at room temperature (20–25 °C) for 24 h and from mononuclear cells stored at −150 °C. Therefore, transported samples can be easily used for generating iPSCs in any clinical situation. SeV also has the possibility to be used for generating iPSCs from other human blood cells such as monocytes, which, on the basis of existing reports of iPSCs that were generated successfully using SeV from T cells and $CD34^+$ cells[7,10], do not harbor T cell receptor (TCR) or immunoglobulin gene rearrangements.

Comparison with other methods

In the first report of iPSC generation from human peripheral blood cells[6], mobilized $CD34^+$ human peripheral blood cells were successfully reprogrammed into iPSCs. However, this method required extremely large amounts (~300 ml) of blood, an apheresis machine and drug administration before blood sampling to mobilize the $CD34^+$ blood cells, all of which should ideally be avoided because of the possible associated side effects (e.g., bone pain), despite these effects being infrequent. Less invasive methods using peripheral blood have also been reported for

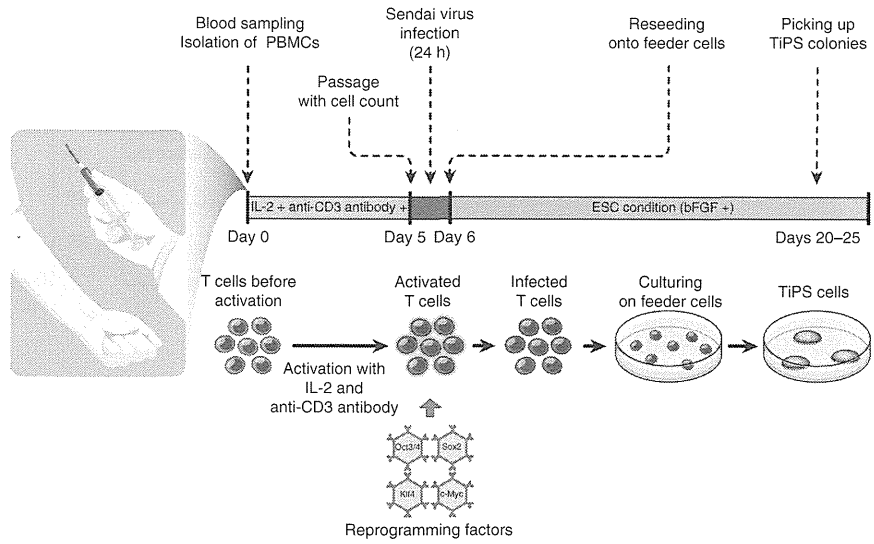

Figure 1 | Overview of the TiPSC generation protocol. PBMCs are activated for 5 d with IL-2 and anti-CD3 antibody, and then transduced with SeV expressing human *OCT3/4, SOX2, KLF4* and *c-MYC*. TiPSC colonies emerge at 20–25 d after blood sampling.

the successful reprogramming of mononuclear blood cells[15–17]. In these methods, mononuclear blood cells from donors or frozen samples were infected using retrovirus[15] or lentivirus[16,17] to express four factors, human OCT3/4, SOX2, KLF4 and c-MYC. In these studies, human T cell reprogramming into iPSCs was achieved, but the efficiency of reprogramming was extremely low (approximately 0.0008–0.01%). Although these methods used less peripheral blood and did not require the pharmacological pretreatment of patients, the problems of transgene genomic insertion and low reprogramming efficiency remained, precluding their wide use in the clinical application of iPSCs. Generating iPSCs with TS-mutated SeV easily erases residual genomic viral RNA from the target cells[10], and the method is significantly more efficient (~0.1%) compared with those protocols in which iPSCs were generated from T cells with retrovirus or lentivirus.

Human keratinocytes derived from plucked human hair have also been used as another less invasive method of obtaining iPSCs from patient cells[4,18]. However, in some cases, these reported methods require several hairs to obtain successful cell outgrowth of keratinocytes. Dental tissue has also been explored as a potential source of iPSCs[19]. However, although teeth are routinely removed in many clinics and no further procedures are required with respect to the donor, it is generally difficult to routinely obtain patients' dental tissues—with specific genetic or nongenetic diseases—for the purpose of iPSC studies. In comparison with these outlined methods, our protocol involves harvesting only a small sample of peripheral blood; in addition, T cell proliferation does not need stochastic cell outgrowth. These are clear advantages for clinical application in comparison with the methods reported in the past.

Experimental design

Blood sampling. Our protocol is focused on the simple procedure of peripheral venous blood sampling to obtain the donor cells, using a standard process. Patient somatic cells can then be easily and aseptically obtained from the blood sample. In our protocol, 1 ml of whole blood is sufficient to generate TiPSCs (**Fig. 2a**).

Derivation of activated T cells. Peripheral blood mononuclear cells (PBMCs) can be separated by a Ficoll gradient method from heparinized whole blood samples (**Fig. 2b**). Although PBMCs contain lymphocytes and monocytes, activation with plate-bound anti-CD3 monoclonal antibody and IL-2 selectively proliferates T cells, and clearly increases the proportion of T cells in the cultured PBMCs[11]. CD3 protein exists in the complex of TCR proteins on the surface of T cells, and can therefore be used as a T cell–specific marker. Anti-CD3 antibody modulates the TCR-CD3 complex to induce T cell proliferation and activation[20], whereas IL-2 also activates general T cell signaling pathways and eventually promotes cytokine transcription, cell survival, cell-cycle entry and growth[21]. At day 5 of culture with anti-CD3 monoclonal antibody and IL-2, $CD3^+$ cells increased up to ~95% of cultured PBMCs (**Fig. 2c–e**). With this culture method, users can avoid using a fluorescence-activated cell sorter in which

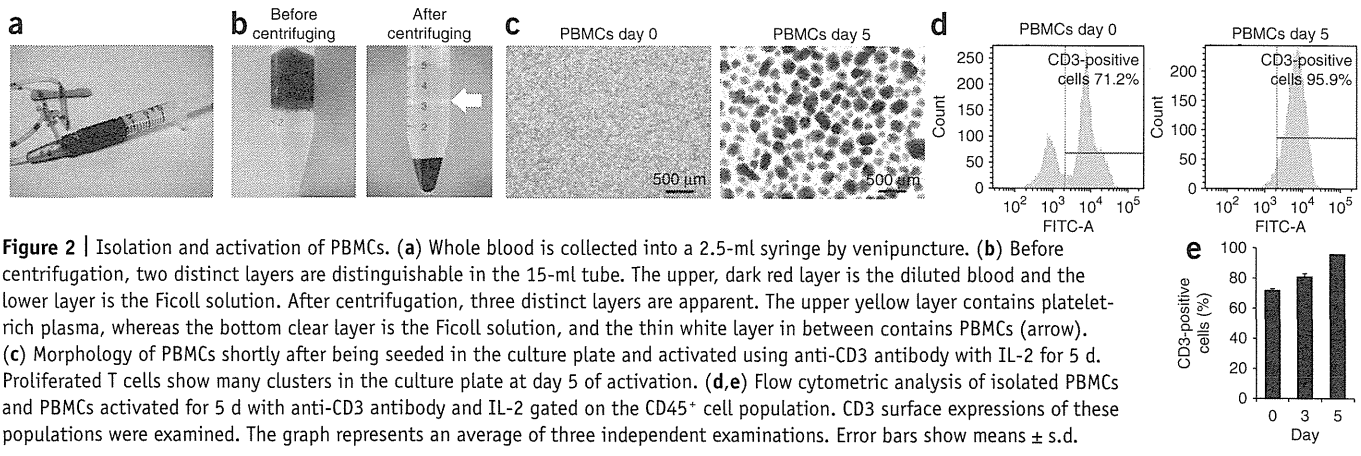

Figure 2 | Isolation and activation of PBMCs. (**a**) Whole blood is collected into a 2.5-ml syringe by venipuncture. (**b**) Before centrifugation, two distinct layers are distinguishable in the 15-ml tube. The upper, dark red layer is the diluted blood and the lower layer is the Ficoll solution. After centrifugation, three distinct layers are apparent. The upper yellow layer contains platelet-rich plasma, whereas the bottom clear layer is the Ficoll solution, and the thin white layer in between contains PBMCs (arrow). (**c**) Morphology of PBMCs shortly after being seeded in the culture plate and activated using anti-CD3 antibody with IL-2 for 5 d. Proliferated T cells show many clusters in the culture plate at day 5 of activation. (**d**,**e**) Flow cytometric analysis of isolated PBMCs and PBMCs activated for 5 d with anti-CD3 antibody and IL-2 gated on the $CD45^+$ cell population. CD3 surface expressions of these populations were examined. The graph represents an average of three independent examinations. Error bars show means ± s.d.

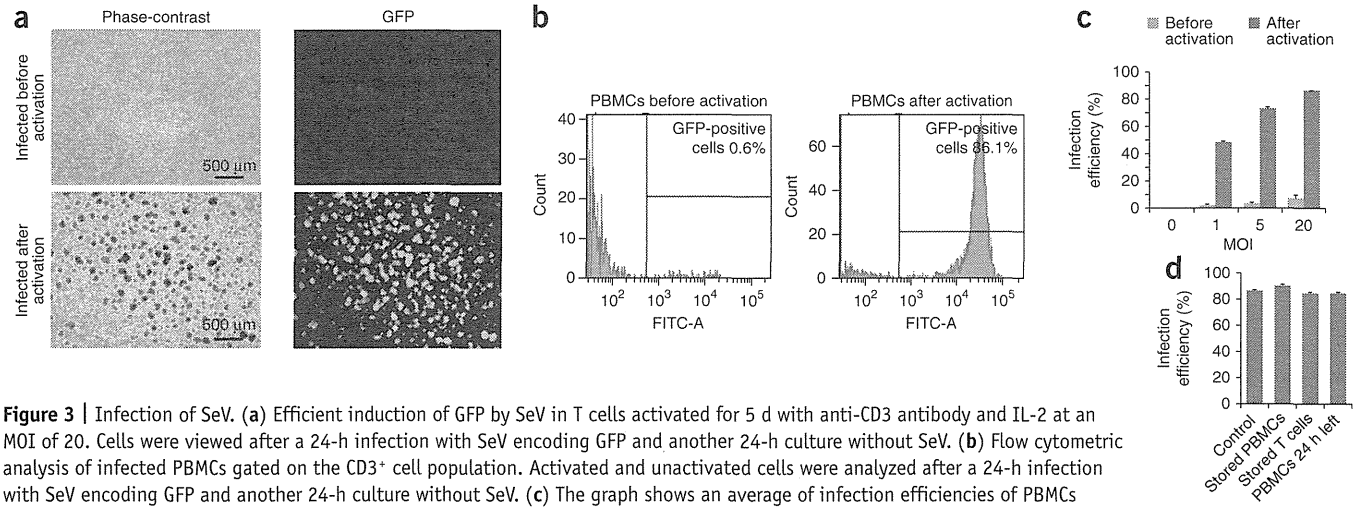

Figure 3 | Infection of SeV. (**a**) Efficient induction of GFP by SeV in T cells activated for 5 d with anti-CD3 antibody and IL-2 at an MOI of 20. Cells were viewed after a 24-h infection with SeV encoding GFP and another 24-h culture without SeV. (**b**) Flow cytometric analysis of infected PBMCs gated on the $CD3^+$ cell population. Activated and unactivated cells were analyzed after a 24-h infection with SeV encoding GFP and another 24-h culture without SeV. (**c**) The graph shows an average of infection efficiencies of PBMCs gated on the $CD3^+$ cell population. Activated and unactivated cells were analyzed after a 24-h infection with SeV encoding GFP and another 24-h culture without SeV. An average of three independent examinations are represented. Error bars show means ± s.d. (**d**) The graph shows an average of infection efficiencies of SeV to activated PBMCs obtained from the frozen stocks of PBMCs, frozen stock of already activated PBMCs and whole blood stored for 24 h before use. These cells were infected for 24 h with SeV encoding GFP at an MOI of 20. Analyses were done after another 24 h of culture without SeV. Flow cytometric analysis of the cells gated on the $CD3^+$ cell population in three independent examinations is shown. Error bars show means ± s.d.

the sorted cells are frequently damaged by laser emission and the process of single-cell sorting.

Introduction of SeV vectors. SeV is an enveloped virus with a single-stranded, negative-sense, nonsegmented RNA genome belonging to the paramyxoviridae family. Recombinant SeV vectors replicate only in the cytoplasm of infected cells[9]. SeV vectors containing reprogramming factors were generated by introducing open reading frames for the human *OCT3/4* (official symbol: *POU5F1*) *SOX2* and *KLF4* genes into a fusion protein (F)-deficient, TS SeV vector. SeV vector containing the *c-MYC* gene was also generated with a more TS mutant, the TS15-SeV vector (P2, L1361C, L1558I), so that it could be eliminated rapidly at 37 °C[10].

The seed SeV/ΔF vectors are generated by the transfecting template pSeV/ΔF carrying each transgene and pCAGGS plasmids—varying the genes encoding T7 RNA polymerase, nucleoprotein (NP), phosphoprotein (P), F5R and large protein (L)—into 293T cells. Thereafter, the vector is propagated using LLC-MK2/F7/A cells, which are SeV F–expressing LLC-MK2 cells[10]. SeV solutions can be stored at −80 °C and thawed before use. Activated PBMCs are infected at day 5 of activation culture. For effective reprogramming of T cells, this activation of PBMCs is important because it not only increases the number of T cells, but also significantly promotes the introduction efficiency of SeV. At a multiplicity of infection (MOI) of 20, SeV could infect $CD3^+$ T cells at >80% efficiency, which was lower than 10% before activation (**Fig. 3**).

TiPSCs

At around day 15 after transduction of SeV, human embryonic stem cell (ESC)-like colonies emerge on the feeder cells (**Fig. 4**). These T cell–derived TiPSC colonies show monoclonal TCR rearrangement in their genome, which is a hallmark of mature terminally differentiated T cells and indicates that each TiPSC colony is derived from a single mature T cell.

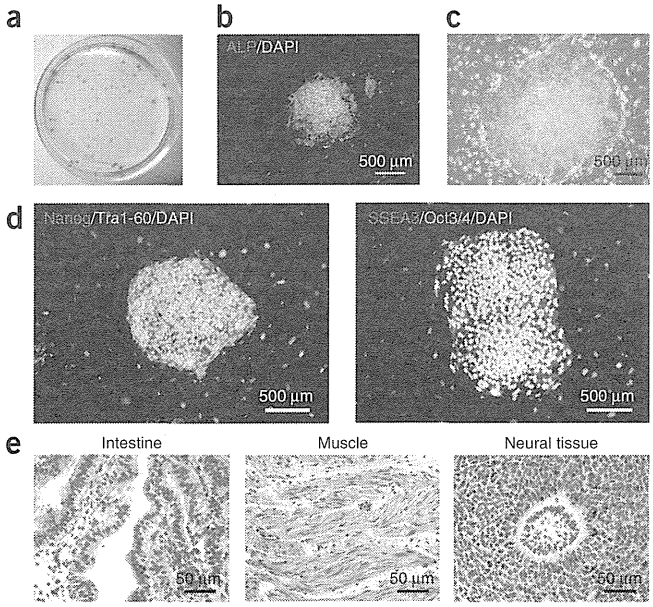

Figure 4 | Characterization of TiPSCs. (**a**) Example of a 10-cm dish stained for ALP on day 20 after SeV infection at an MOI of 20 and seeded at a density of 5×10^4 cells per 10-cm dish. Many ALP-positive T cell colonies that were infected with SeV are visible. (**b**) ALP staining of TiPSC colonies. (**c**) Typical ESC-like TiPS colony on day 20 after SeV infection. (**d**) Immunofluorescense staining for pluripotency and surface markers (Nanog, Tra1-60, Oct 3/4, SSEA3) in TiPSCs. Immunofluorescence staining was performed using the following primary antibodies: anti-NANOG (RCAB0003P, ReproCELL), anti-OCT3/4 (sc-5279, Santa Cruz), anti-SSEA3 (MAB4303, Millipore) and anti-Tra1-60 (MAB4360, Millipore). DAPI (Molecular Probes) was used for nuclear staining. The following secondary antibodies were used: anti-rabbit IgG and anti-mouse IgG and IgM conjugated with Alexa Fluor 488 or Alexa Fluor 568 (Molecular Probes). (**e**) Hematoxylin and eosin–stained representative teratomas derived from the TiPSC line.

MATERIALS

REAGENTS

- Donors for blood sampling ! CAUTION Subjects must have given informed consent. ! CAUTION All experiments involving humans must conform to relevant governmental and institutional ethics regulations.
- Novo-heparin (5,000 units per 5 ml; Mochida Pharmaceutical)
- Ficoll-Paque PREMIUM (GE Healthcare, cat. no. 17-5442-02)
- Purified NA/LE mouse anti-human CD3 (BD Pharmingen, cat. no.555336)
- GT-T502 medium (Kohjin Bio, cat. no. 16025020)
- Fetal bovine serum (FBS; Cell Culture Bioscience, cat. no. 171012)
- Bovine albumin fraction V solution (BSA; Gibco, cat. no. 15260-037)
- DMEM (Sigma, cat. no. D5546)
- DMEM/F12 (Sigma, cat. no. D6421)
- KnockOut serum replacement for ESCs/iPSCs (KSR; Gibco, cat. no. 10828-028)
- GlutaMAX-I (Gibco, cat. no. 35050-061)
- Non-essential amino acid solution (NEAA; Sigma, cat. no. M7145)
- Penicillin-streptomycin (Gibco, cat. no. 15140-122)
- 2-Mercaptoethanol (2-ME; Invitrogen, cat. no. 21985-023)
  ! CAUTION This solution is flammable, harmful if swallowed and toxic when in contact with skin and eyes. Use protective gloves and safety glasses when handling it.
- Recombinant basic fibroblast growth factor, human (bFGF; Wako, cat. no. 064-04541)
- Collagenase type IV (Gibco, cat. no. 17104-019)
- Gelatin powder (Sigma, cat. no. G-1890)
- D-PBS(−) (Wako, cat. no. 045-29795)
- Acetamide (Wako, cat. no. 015-00115)
- Propylene glycol (Wako, cat. no. 16-0499)
- Cell Banker-2 (BIO LABO, cat. no. BLC-2)
- TRIzol reagent (Invitrogen, cat. no. 15596-026)
- Chloroform (Wako, cat. no. 038-02606)
- Ethanol (Wako, cat. no. 057-00456)
- Ethanol (70% (vol/vol); Wako, cat. no. 059-07895)
- Isopropyl alcohol (Wako, cat. no. 166-04836)
- SuperScript double-stranded cDNA synthesis kit (Invitrogen, cat. no. 11917-010)
- Oligo $(dT)_{12-18}$ primer (Invitrogen, cat. no. 18418-012)
- SYBR Premix Ex Taq II (Takara, cat. no. RR081A)
- Sodium acetate (3 M; Wako, cat. no. 316-90081)
- Liquid nitrogen
- CytoTune-iPS reprogramming kit (*OCT3/4*-SeV/TSΔF, *SOX2*-SeV/TSΔF, *KLF4*-SeV/TSΔF, *c-MYC (HNL)*-SeV/TS15ΔF; Invitrogen, cat. no. A13780-01)
- Mitomycin C–treated mouse embryonic fibroblasts (MEFs; Reprocell, cat. no. RCHEFC003)
- MEF medium (see REAGENT SETUP)
- Human iPSC medium (see REAGENT SETUP)
- Isopropanol (Wako, cat. no. 16604836)
- RNase-free water (Takara, cat. no. 9012)
- DNase I (Invitrogen, cat. no. 18068-015)

EQUIPMENT

- Syringe (2.5 ml; Terumo, cat. no. SS-02LZ)
- Butterfly needle (23 G; Terumo, cat. no. SV-23CLK)
- Needle (23 G; Terumo, cat. no. NN-2325R)
- Alcohol prep pads (Hakujuji)
- Tourniquet (Asone, cat. no. MH-01)
- Millex GV filter unit (0.22 μm; Millipore, cat. no. SLGV033RS)
- C-chip disposable hemocytometer (Digital Bio, cat. no. DHC-N01)
- Trypan blue stain (0.4%; Gibco, cat. no. 15250)
- Microtubes (1.5 ml; Thermo Fisher Scientific, cat. no. 131-615C)
- Tube (50 ml; Corning, cat. no. 430829)
- Tube (15 ml; Corning, cat. no. 430053)
- Tissue culture dish (10 cm; Falcon, cat. no. 353003)
- Tissue culture plate (96 well; Falcon, cat. no. 353078)
- Tissue culture plate (24 well; Falcon, cat. no. 353047)
- Tissue culture plate (12 well; Falcon, cat. no. 353043)
- Tissue culture plate (6 well; Falcon, cat. no. 353046)
- Cryovials (1.5 ml; Sumilom, cat. no. MS-4702X)
- Freezing container (Sanyo, cat. no. MDM-U73V)
- Cell culture incubator set at 37 °C, 5% CO_2 (Sanyo, cat. no. MCO-18AIC)
- Versatile refrigerated centrifuge (Sanyo, cat. no. AX-320)
- NanoDrop 2000 (Thermo Fisher Scientific, cat. no. ND-2000)
- ABI 7500 real-time PCR system (Applied Biosystems, cat. no. 7500-01)
- Inverted microscope
- Phase-contrast microscope

REAGENT SETUP

bFGF Prepare 0.1% (wt/vol) BSA/PBS in a sterile tube and use it to dissolve bFGF for a final concentration of 4 ng ml^{-1}. Prepare 100-μl aliquots in screw-cap microcentrifuge tubes and store them at −20 °C.

Gelatin-coated culture dishes Dissolve 1 g of gelatin powder in 1,000 ml of distilled water, autoclave, filter the solution with a 0.22-μm Millex GV filter unit and store it at 4 °C. Add an appropriate volume of 0.1% (wt/vol) gelatin solution to cover the entire area of the culture dishes to coat. Incubate the dishes for at least 30 min at 37 °C in a sterile environment. Remove the gelatin solution before use.

Collagenase type IV solution Dissolve 1 g of collagenase type IV powder in 1,000 ml of DMEM/F12 medium and filter the solution with a 0.22-μm Millex GV filter unit. Make 50-ml aliquots in 50-ml tubes and store them at −20 °C. Thawed solution can be stored at 4 °C for up to 1 week before use.

Anti-CD3 monoclonal antibody–coated plates Dissolve anti-human CD3 antibody in D-PBS(−) to a concentration of 10 μg ml^{-1}. Add the anti-human CD3 antibody solution to 24-well tissue culture plates to soak the surface of each plate, and then incubate them at 37 °C in a 5% CO_2 incubator for at least 30 min. Remove the anti-human CD3 antibody solution and wash the plates once with D-PBS(−) before seeding the cells.

Human iPSC medium To prepare 500 ml of human iPSC medium, mix 387.5 ml of DMEM/F12 medium with 100 ml of KSR, 5 ml of GlutaMAX-I (1 mM), 5 ml of penicillin-streptomycin, 5 ml of NEAA (10 μM), 500 μl of 2-ME (100 μM) and 50 μl of bFGF (4 ng ml^{-1}). Filter the medium with a 0.22-μm filter unit and store it for up to 1 week at 4 °C.

MEF medium To prepare 500 ml of MEF medium, mix 450 ml of DMEM medium with 50 ml of FBS and 2.5 ml of penicillin-streptomycin. Filter the medium with a 0.22-μm filter unit and store it for up to 2 weeks at 4 °C.

DAP213 solution To prepare 10 ml of DAP213 solution, mix 5.37 ml of human iPSC medium, 1.43 ml DMSO, 1 ml of 10 M acetamide and 2.2 ml of propylene glycol. Store the solution for up to 1 month at −80 °C.

SeV solutions To prepare working stocks of SeV solutions (from the CytoTune kit), thaw the solutions on ice and prepare 50-μl stocks in 1.5-ml tubes. Working stocks can be stored at −80 °C.

PROCEDURE

Blood sampling ● TIMING ~10 min

1| Sterilize the cap from the bottle of heparin with an alcohol prep pad.

! CAUTION Wash your hands before starting venipuncture. Wear gloves when handling blood. Change gloves after venipuncture in each donor or if the gloves become contaminated.

2| Combine a 23-G needle and 2.5-ml syringe and draw up 100–300 μl of heparin.

3| Release the 23-G needle from heparinized 2.5-ml syringe and combine a new 23-G butterfly needle with the heparinized 2.5-ml syringe.

4| Identify the median cubital or cephalic veins of donors' arms; then palpate and trace the vein paths with the index finger.

5| Sterilize the venipuncture site with an alcohol prep pad.
! CAUTION Do not palpate the venipuncture site after sterilization.

6| Apply the tourniquet above the selected puncture site.
! CAUTION Do not place the tourniquet too tightly or leave it on for more than 3 min.

7| Remove the needle shield and perform venipuncture. Insert the needle into the blood vessel and hold still once a backflow of blood is seen in the tube of the butterfly needle setup.
! CAUTION Venipuncture must be done by a person who is well trained and legally certified to carry out the procedure.
! CAUTION Patients' informed consent must be obtained before blood sampling.

8| Draw 1–2 ml of blood into the syringe.

9| Remove the tourniquet.
! CAUTION Do not withdraw the needle before removing the tourniquet.

10| Withdraw the needle fully, apply pressure to the alcohol prep pad over the puncture site and maintain the pressure for 3–5 min until the bleeding stops.

11| Discard the needle of the Vacutainer into a biohazard container without recapping the needle.
! CAUTION Dispose of items that are used for venipuncture immediately and in appropriate containers.
▲ CRITICAL STEP This step and all subsequent steps should be carried out using sterile reagents and equipment.
■ PAUSE POINT Heparinized whole blood can be stored for up to 24 h before use (**Fig. 2a**).

Isolating PBMCs using Ficoll gradient ● TIMING ~1 h

12| Add 1–2 ml of heparinized whole blood to a 15-ml tube.
? TROUBLESHOOTING

13| Add 1–2 ml of D-PBS(−) and dilute the blood with D-PBS(−) 1:1.

14| Prepare 3 ml of Ficoll-Paque PREMIUM in a separate 15-ml tube.

15| Pour the diluted blood onto the Ficoll solution carefully so as to form two layers.
! CAUTION Do not mix the blood and the Ficoll solution. The blood must remain on top.

16| Centrifuge for 30 min at 400*g* at room temperature.

17| Collect the layer of PBMCs without touching the Ficoll layer, using sterile pipette tips, into a new 15-ml tube (**Fig. 2b**).
▲ CRITICAL STEP When collecting PBMCs, carefully avoid obtaining any of the Ficoll solution layer. Contamination of the Ficoll solution reduces the collection rate of the mononuclear cells.

18| Dilute the PBMCs by adding 5 ml of D-PBS(−).

19| Centrifuge for 5 min at 200*g* at room temperature.

20| Discard the supernatant, add 5 ml of D-PBS(−) and dilute the PBMCs with D-PBS(−).

21| Centrifuge for 5 min at 200*g* at room temperature.

22| Discard the supernatant and resuspend the PBMCs with GT-T502 medium to a concentration of 1.25×10^6 cells per ml.
■ **PAUSE POINT** If needed, isolated PBMCs can be frozen and stored at −150 °C by using Cell Banker-2 according to the manufacturer's instructions.

Activating T cells ● TIMING 5 d

23| Add 400 µl of PBMC solution with GT-T502 medium into the wells of a human CD3-specific antibody–coated 24-well plate at a density of 5×10^5 cells per well.
▲ **CRITICAL STEP** Approximately 1 to 2×10^6 PBMCs can be obtained from 1 ml of human peripheral blood with a Ficoll gradient method. This number of PBMCs fills 2–4 wells of a standard 24-well plate. For TiPSC generation, one well of PBMCs is sufficient. Excess cells can be stored using Cell Banker-2, as described at the **PAUSE POINT** in Step 22.

24| Incubate the cells for 5 d at 37 °C in a 5% CO_2 incubator without medium change.
■ **PAUSE POINT** If needed, activated PBMCs can be frozen and stored at −150 °C by using Cell Banker-2 according to the manufacturer's instructions.

SeV infection ● TIMING ~1 d

25| Dilute the SeV solutions containing *OCT3/4*-SeV/TSΔF, *SOX2*-SeV/TSΔF, *KLF4*-SeV/TSΔF and *c-MYC (HNL)*-SeV/TS15ΔF individually on ice as detailed in REAGENT SETUP. This will take ~30 min.
! **CAUTION** Perform all procedures involving SeV vectors in a safety cabinet while wearing gloves. All waste should be treated first with ethanol, then with bleach, and finally it should be autoclaved.

26| Collect the activated PBMCs by pipetting and transfer them into a 15-ml tube.

27| Centrifuge for 5 min at 200*g* at room temperature.

28| Discard the supernatant and resuspend the cells with GT-T502 medium to a concentration of 7.5×10^5 cells per ml.

29| Add 1 ml of PBMC solution with GT-T502 medium into the wells of a human CD3-specific antibody–coated 12-well plate at a density of 7.5×10^5 cells per well.
▲ **CRITICAL STEP** After 5 d of activation with CD3-specific antibody and IL-2, approximately twofold amounts of activated PBMCs should be obtained. This amount of activated PBMCs fills 2–5 wells of a standard 12-well plate. For TiPSC generation, one well of activated PBMCs is sufficient. Excess cells can be stored using Cell Banker-2.
■ **PAUSE POINT** If needed, activated PBMCs can be frozen and stored at −150 °C by using Cell Banker-2 according to the manufacturer's instructions.

30| Add the virus solutions containing *OCT3/4*-SeV/TSΔF, *SOX2*-SeV/TSΔF, *KLF4*-SeV/TSΔF and *c-MYC (HNL)*-SeV/TS15ΔF individually to the wells, each at an MOI of 20. One well containing all virus solutions is sufficient to generate TiPS colonies.

31| Place the plate in an incubator at 37 °C and 5% CO_2. This plate should be left undisturbed for 24 h for cells to grow; meanwhile, however, immediately proceed with Step 32 (MEF plating).

Plating MEFs ● TIMING ~30 min

32| Place 10 ml of MEF medium in a 50-ml tube. Although MEFs should be ready for use on the following day, plating of MEFs should be done 1 d before plating infected PBMCs for optimal cell viability.

33| Remove a vial of frozen MEFs from freezing container and place the vial into a 37 °C water bath until thawed.

34| Wipe the vial with ethanol, open the cap and transfer the cell suspension to the tube prepared in Step 32.

35| Centrifuge the tube for 5 min at 200*g* at room temperature.
? TROUBLESHOOTING

36| Discard the supernatant and resuspend the cells with 50 ml of MEF medium.

37| Add 10 ml of MEF suspension onto a 10-cm gelatin-coated dish, or add 2 ml into each well of a gelatin-coated six-well plate (6×10^6 cells per 10-cm dish or 1.2×10^5 cells per well of a six-well plate).

38| Incubate overnight at 37 °C in a 5% CO_2 incubator.
■ PAUSE POINT The MEF dishes can be stored for up to 3–4 d before use.

Replating infected PBMCs ● TIMING ~30 min
39| Collect the infected cells (from Step 31) by pipetting and transfer them into a 15-ml tube.

40| Centrifuge for 5 min at 200*g* at room temperature.

41| Discard the supernatant and resuspend the cells with 1 ml of human iPSC medium.

42| Aspirate the medium from the 10-cm dishes with MEF feeder cells (prepared in Steps 32–38) and add 10 ml of human iPSC medium into the dishes.

43| Use a hemocytometer to count the number of cells in solution prepared in Step 41 and replate 5×10^4 and 5×10^5 cells on a 10-cm dish with the MEF feeder cells prepared in Step 42.
▲ CRITICAL STEP After 24 h of infection, approximately 1×10^6 PBMCs can be obtained from one well of a 12-well plate. This number of infected PBMCs is sufficient to replate 5×10^4 and 5×10^5 cells on a 10-cm dish with MEF feeder cells.
▲ CRITICAL STEP Excess infected PBMCs can be used as a positive control for assessing the removal of SeV by real-time PCR. Dilute 5×10^4 cells of infected PBMCs with 500 μl of TRIzol and store it at −80 °C if needed.

44| Incubate the dish at 37 °C in a 5% CO_2 incubator.

Culturing infected PBMCs ● TIMING ~3 weeks
45| After replating the infected mononuclear cells, change the human iPSC medium every 2 d and maintain cells in culture until the TiPSC colonies emerge.
▲ CRITICAL STEP The infected mononuclear cells should be attached to the MEFs within the first 2 d after replating. It is not a problem for TiPSCs generation if unattached cells are lost when changing the human iPSC medium.

46| About 10 d after replating, small colonies should start to appear. At about 15–20 d after replating, colonies showing typical human ESC colony-like morphology should emerge (**Fig. 4c**).

Picking up and expanding the TiPSC colonies ● TIMING ~3 weeks
47| Mark the colonies that show ESC-like morphology on the bottom of the dish under an inverted microscope.

48| Prepare the required number of six-well plates with MEF feeder cells.

49| Replace the medium in the six-well plates with MEF feeder cells by human iPSC medium at the amount of 2 ml per well.

50| Add 20 μl of human iPSC medium into the required number of wells of 96-well plates. Colony pick-up needs one well per colony.
? TROUBLESHOOTING

51| Wipe a phase-contrast microscope carefully with ethanol and place it onto a tissue culture clean bench.

52| By using the phase-contrast microscope and a 20-μl pipette, pick up the colonies marked in Step 36 and place each colony into one well of the 96-well plates containing human iPS cell medium (added in Step 50).

53| Use a phase-contrast microscope and a 200-μl pipette to add 200 μl of human iPSC medium into the wells of 96-well plates and break the colonies into small pieces by pipetting.
! CAUTION Do not disperse the colonies into single cells.

54| Transfer the broken colonies into wells of six-well plates containing MEF feeder cells as prepared in Step 48.

55| Incubate at 37 °C in a 5% CO_2 incubator. Change human iPSC medium every 2 d.

56| Every 5–7 d, passage the cells by using collagenase IV solution as follows: when the colonies become confluent, aspirate the medium and add collagenase IV solution (use half the amount you use for maintenance medium; for example, 1 ml for a well of a six-well plate and 5 ml for a 10-cm dish).

57| Incubate for 30–60 min at 37 °C in a 5% CO_2 incubator.

58| Collect the colonies into a 15-ml tube by pipetting when floating colonies appear.

59| Centrifuge for 2 min at 200*g* at room temperature.

60| Discard the supernatant. Add 1 ml of fresh human iPSC medium and break the colonies into small pieces with a 1,000-μl pipette and by pipetting 1 ml of cell solution four or five times.
! **CAUTION** Do not disperse the colonies into single cells.

61| Place the broken colonies into a new dish or plate that has been pre-plated with MEFs and filled with fresh human iPS culture medium. The split ratio used for the cells depends on the cell lines and usually ranges from 1:4 to 1:10.

62| If you wish to freeze the iPSCs, follow option A. If you wish to check for the removal of SeV by real-time RT-PCR, follow option B.

(A) Freezing of iPSCs ● TIMING **~1 h**

(i) Aspirate the medium and add collagenase IV solution as detailed in Step 56.
(ii) Incubate for 30–60 min at 37 °C in a 5% CO_2 incubator.
(iii) Collect the colonies into a 15-ml tube by pipetting when floating colonies appear.
(iv) Centrifuge for 2 min at 200*g* at room temperature.
(v) Discard the supernatant, add 200 μl of DAP213 solution and break the colonies into small pieces with a 200-μl pipette.
! **CAUTION** For good cell viability, perform this step and Steps 62A(vi) and Steps 62A(vii) within 15 s.
(vi) Transfer 200 μl of the cell suspension to 1.5-ml cryovials.
(vii) Plunge the vials quickly into liquid nitrogen.
(viii) Store the cryovials in the freezing container at −150 °C.

(B) Checking for removal of SeV by real-time RT-PCR ● TIMING **~8 h**

(i) Prepare primers as shown in **Table 1**.
(ii) Transfer the excess broken colonies from Step 50 into 1.5-ml tubes. Half of the cells from a 10-cm dish of confluent TiPSCs will supply sufficient mRNA.
(iii) Centrifuge for 2 min at 200*g* at room temperature.
(iv) Discard the supernatant. Dilute the broken colonies by adding 1 ml of D-PBS(−).
(v) Centrifuge for 2 min at 200*g* at room temperature.
(vi) Discard the supernatant. Dilute the broken colonies by adding 500 μl of TRIzol.
■ **PAUSE POINT** Cell lysates prepared with TRIzol should be stored at −80 °C.
(vii) Add 100 μl of chloroform to 500 μl of cell lysate (which should be thawed on ice if stored at −80 °C) and mix vigorously by shaking. To make a positive control, thaw the infected PBMC lysate prepared in Step 43 on ice and use protocol (viii–xxxv) with infected PBMC lysate, as was used for the TiPSC samples.

TABLE 1 | Primer sequences for detecting SeV.

Primers	Sense	Antisense
SeV-hOct3/4	5′-TCTGGGCTCTCCCATGCATTCAAAC-3′	5′-AATGTATCGAAGGTGCTCAA-3′
SeV-hSox2	5′-ACGGCCATTAACGGCACACTG-3′	5′-AATGTATCGAAGGTGCTCAA-3′
SeV-hKlf4	5′-CACCTCGCCTTACACATGAAGAG-3′	5′-AATGTATCGAAGGTGCTCAA-3′
SeV-c-Myc	5′-TAACTGACTAGCAGGCTTGTCG-3′	5′-AAATACGGCTGCACCGAGTCGT-3′
GAPDH	5′-GTGGACCTGACCTGCCGTCT-3′	5′-GGAGGAGTGGGTGTCGCTGT-3′

(viii) Centrifuge for 15 min at 12,000*g* at 4 °C.
(ix) Transfer the aqueous phase (200–250 μl) of lysate to a new 1.5-ml microtube.
(x) Add 250 μl of isopropanol to the lysate transferred in Step 58 and mix well by pipetting several times.
(xi) Centrifuge for 5 min at 12,000*g* at 4 °C.
(xii) Remove the supernatant and add 500 μl of 70% (vol/vol) ethanol.
(xiii) Centrifuge for 2 min at 9,000*g* at 4 °C.
(xiv) Remove the ethanol completely and air-dry the pellet at room temperature for 5 min.
(xv) Resuspend the pellet in 50 μl of RNase-free water.
(xvi) Use 2 μl of the sample to determine the RNA concentration of samples by measuring with an optical spectrometer (NanoDrop), and adjust the concentration of each sample to 20 ng μl^{-1} by adding RNase-free water.
(xvii) Transfer 100 μl of lysate (which contains 2 μg of RNA) to a new 1.5-ml microtube.
(xviii) Add 250 μl of ethanol and 10 μl of 3 M sodium acetate, and then mix vigorously by shaking.
(xix) Refrigerate the lysate at −20 °C for 30 min.
(xx) Centrifuge for 15 min at 12,000*g* at 4 °C.
(xxi) Remove the supernatant and add 500 μl of 70% (vol/vol) ethanol.
(xxii) Centrifuge for 2 min at 9,000*g* at 4 °C.
(xxiii) Remove the ethanol completely and air-dry the pellet at room temperature for 5 min.
(xxiv) Resuspend the pellet in 16 μl of RNase-free water.
(xxv) Add 2 μl of 10× DNase I buffer and 2 μl of DNase I to the RNA lysate, mix gently by finger tapping and incubate for 15 min at room temperature.
(xxvi) Add 2 μl of 25 mM EDTA, mix gently by finger tapping and incubate for 10 min at 65 °C.
(xxvii) Transfer the tube onto ice.
(xxviii) Transfer 14 μl of RNA lysate to a new 1.5-ml microtube and then add 2 μl of Oligo dT and 8 μl of 2.5 mM dNTP mix.
(xxix) Incubate for 5 min at 65 °C.
(xxx) Place the tube on ice.
(xxxi) Add 8 μl of 5× first-strand buffer, 4 μl of 0.1 M DTT, 2 μl of 40 U μl^{-1} of RNase inhibitor and 2 μl of SuperScript II.
(xxxii) Mix gently by finger tapping and incubate for 50 min at 42 °C.
(xxxiii) Incubate for 15 min at 70 °C.
■ **PAUSE POINT** cDNA samples should be stored at −20 °C.
(xxxiv) Prepare 20 μl of real-time PCR mixture by mixing the reagents listed below in a 96-well PCR plate.

Real-time PCR mixture	Per tube (μl)
SYBR Premix ExTaq	10
Primer sense (10 μM)	0.4
Primer antisense (10 μM)	0.4
H_2O	4
Rox	0.2
DNA sample	5
Total	20

(xxxv) Perform a SYBR Green reaction in 96-well plates on an ABI 7500 real-time PCR instrument (95 °C, 30 s; 60 °C, 30 s; 72 °C, 30 s).
▲ **CRITICAL STEP** By using a cDNA sample obtained from infected PBMCs as positive control and standards, check the expression of transgenes that were normalized to the expression of GAPDH. Check the expression of TiPSC transgenes after 10–15 passages.

? TROUBLESHOOTING

Troubleshooting advice can be found in **Table 2**.

TABLE 2 | Troubleshooting table.

Step	Problem	Possible reason	Solution
12	The number of PBMCs is insufficient	Ficoll is mixed into the PBMC solution	If more than 1×10^5 cells were obtained, seed them in 400 μl of GT-T502 medium, incubate for 6–7 d, and go to Step 25. If not, repeat Steps 2–12 with new whole blood and collect PBMCs carefully without mixing Ficoll
35	No TiPSC colonies appear	Viral titer is low	Use new SeV solution. Avoid using SeV solution after repeated freeze-thaw cycles
		Most T cells are dead before infection	Ensure the density of T cells in each appropriate step. Try SeV infection on day 4 of activation
50	Signs of iPSC differentiation after expansion	Poor-quality human iPSC medium	Use new human iPSC medium or increase bFGF concentration in the medium

● TIMING

Steps 1–11, blood sampling: ~10 min
Steps 12–22, isolating PBMCs using Ficoll gradient: ~1 h
Steps 23 and 24, activating T cells: 5 d
Steps 25–31, SeV infection: ~1 d
Steps 32–38, plating MEFs: ~30 min
Steps 39–44, replating infected PBMCs: ~30 min
Steps 45 and 46, culturing infected PBMCs: ~3 weeks
Steps 47–62, picking up and expanding the TiPSC colonies: ~3 weeks

ANTICIPATED RESULTS

T cells make up approximately 70% or less of isolated PBMCs, and they are inefficiently infected by SeV vectors before activation. However, after a 5-d activation with IL-2 and anti-CD3 antibody, the T cell proportion increases to become >95% of PBMCs, and it can be effectively infected with SeV vectors. With proper activation, T cells are infected with SeV vectors at >80% efficiency at an MOI of 20 (**Fig. 3a–d**).

From the 5×10^4 cells infected with SeV vectors encoding human OCT3/4, SOX2, KLF4 and c-MYC and seeded onto MEF feeder cells, 50–100 ESC-like colonies grow, on average (**Fig. 4a**). The TiPSC colonies clearly stain positive for alkaline phosphatase (ALP), a stem cell marker (**Fig. 4b**) and express ESC marker transcripts (**Fig. 4d**). The expression of TiPSC transgenes is not always detectable after 10–15 passages. They can also differentiate into three germ layer–derived tissues and generate teratomas *in vivo* (**Fig. 4e**) and embryoid bodies *in vitro*. These TiPSC lines will have TCR rearrangement in their genome, which is a hallmark of mature terminally differentiated T cells, and will show specific peaks for Dβ/Jβ and Vβ/Jβ recombination in capillary electrophoresis of the PCR products.

ACKNOWLEDGMENTS T.S. is a research fellow of the Japan Society for the Promotion of Science. This work was supported in part by research grants from the Ministry of Education, Science and Culture, Japan, and by a grant from the New Energy and Industrial Technology Development Organization.

AUTHOR CONTRIBUTIONS T.S. and S.Y. prepared most of the paper. K.F. provided advice and proofread the paper.

COMPETING FINANCIAL INTERESTS The authors declare no competing financial interests.

Published online at http://www.natureprotocols.com/.
Reprints and permissions information is available online at http://www.nature.com/reprints/index.html.

1. Takahashi, K. & Yamanaka, S. Induction of pluripotent stem cells from mouse embryonic and adult fibroblast cultures by defined factors. *Cell* **126**, 663–676 (2006).
2. Takahashi, K., Okita, K., Nakagawa, M. & Yamanaka, S. Induction of pluripotent stem cells from fibroblast cultures. *Nat. Protoc.* **2**, 3081–3089 (2007).
3. Takahashi, K. *et al.* Induction of pluripotent stem cells from adult human fibroblasts by defined factors. *Cell* **131**, 861–872 (2007).
4. Aasen, T. *et al.* Efficient and rapid generation of induced pluripotent stem cells from human keratinocytes. *Nat. Biotechnol.* **26**, 1276–1284 (2008).
5. Kim, J.B. *et al.* Direct reprogramming of human neural stem cells by *OCT4*. *Nature* **461**, 649–653 (2009).
6. Loh, Y.H. *et al.* Generation of induced pluripotent stem cells from human blood. *Blood* **113**, 5476–5479 (2009).

7. Seki, T. *et al.* Generation of induced pluripotent stem cells from human terminally differentiated circulating T cells. *Cell Stem Cell* **7**, 11–14 (2010).
8. Fusaki, N., Ban, H., Nishiyama, A., Saeki, K. & Hasegawa, M. Efficient induction of transgene-free human pluripotent stem cells using a vector based on Sendai virus, an RNA virus that does not integrate into the host genome. *Proc. Jpn. Acad. Ser. B Phys. Biol. Sci.* **85**, 348–362 (2009).
9. Li, H.O. *et al.* A cytoplasmic RNA vector derived from nontransmissible Sendai virus with efficient gene transfer and expression. *J. Virol.* **74**, 6564–6569 (2000).
10. Ban, H. *et al.* Efficient generation of transgene-free human induced pluripotent stem cells (iPSCs) by temperature-sensitive Sendai virus vectors. *Proc. Natl. Acad. Sci. USA* **108**, 14234–14239 (2011).
11. Desai-Mehta, A., Lu, L., Ramsey-Goldman, R. & Datta, S.K. Hyperexpression of CD40 ligand by B and T cells in human lupus and its role in pathogenic autoantibody production. *J. Clin. Invest.* **97**, 2063–2073 (1996).
12. Eminli, S. *et al.* Differentiation stage determines potential of hematopoietic cells for reprogramming into induced pluripotent stem cells. *Nat. Genet.* **41**, 968–976 (2009).
13. Hong, H. *et al.* Suppression of induced pluripotent stem cell generation by the p53-p21 pathway. *Nature* **460**, 1132–1135 (2009).
14. Okano, S. *et al.* Recombinant Sendai virus vectors for activated T lymphocytes. *Gene Ther.* **10**, 1381–1391 (2003).
15. Brown, M.E. *et al.* Derivation of induced pluripotent stem cells from human peripheral blood T lymphocytes. *PLoS ONE* **5**, e11373 (2010).
16. Loh, Y.H. *et al.* Reprogramming of T cells from human peripheral blood. *Cell Stem Cell* **7**, 15–19 (2010).
17. Staerk, J. *et al.* Reprogramming of human peripheral blood cells to induced pluripotent stem cells. *Cell Stem Cell* **7**, 20–24 (2010).
18. Aasen, T. & Belmonte, J.C. Isolation and cultivation of human keratinocytes from skin or plucked hair for the generation of induced pluripotent stem cells. *Nat. Protoc.* **5**, 371–382 (2010).
19. Yan, X. *et al.* iPS cells reprogrammed from human mesenchymal-like stem/progenitor cells of dental tissue origin. *Stem Cells Dev.* **19**, 469–480 (2010).
20. Smith-Garvin, J.E., Koretzky, G.A. & Jordan, M.S. T cell activation. *Annu. Rev. Immunol.* **27**, 591–619 (2009).
21. Lan, R.Y., Selmi, C. & Gershwin, M.E. The regulatory, inflammatory, and T cell programming roles of interleukin-2 (IL-2). *J. Autoimmun.* **31**, 7–12 (2008).